# FINITE ELEMENT ANALYSIS OF PLASTICITY– INDUCED FATIGUE CRACK CLOSURE

by

Mehmet Gökhan Gökçen

B.S., Mechanical Engineering, Boğaziçi University, 1996

M.S., Mechanical Engineering, Boğaziçi University, 1999

Submitted to the Institute for Graduate Studies in
Science and Engineering in partial fulfillment of
the requirements for the degree of
Doctor of Philosophy

Graduate Program in Mechanical Engineering

Boğaziçi University

2006

# ACKNOWLEDGEMENTS

I would like to express my sincere gratitude to Assoc. Prof. Vahan Kalenderoğlu, who has supervised my thesis, for his invaluable guidance and support, and also to Prof. Öktem Vardar for his suggestions and interest during this thesis work. I would also like to thank to members of the dissertation committee Prof. Turan Özturan, Assoc. Prof. Fazıl Önder Sönmez, Assist. Prof. Emre Aksan for their interest.

I would like to thank to my family for their love and support.

# ABSTRACT

Contact elements are implemented into the elastic plastic finite element analysis of fatigue crack closure to predict crack opening stress values, by developing a code using ANSYS Parametric Design Language(APDL). In spite of the fact that the use of contact elements in modeling crack surface contact, and thus in modeling of crack closure is inherently natural, almost no effort to incorporate it in the finite element analysis of fatigue crack growth has been reported in the literature. The traditional method is based on placing truss elements on the crack surface nodes. Their stiffness is set to either zero or to a high value according to the state of the crack to model crack surface contact. The load is applied incrementally, during which the crack surface nodes are monitored to predict crack opening stress values. In this research contact elements are used to model crack surface contact and similar to mentioned method the determination of crack opening stress is accomplished by monitoring the state of contact elements during incrementally applied loading. The results of two dimensional plane strain finite element analyses of center cracked geometry are in good agreement with previous work given in the literature. Instead of determining crack opening stress of every load cycle, an algorithm that makes it possible to find crack opening stress at predetermined load cycle intervals is developed. With the developed algorithm it was possible to analyze crack closure behavior during a larger number of load cycles with less execution time. The newly introduced parameters such as effect of the number increments of the applied load, the effect of the load cycle interval where the opening stress values are determined are investigated. Due to simulation of relatively high number of load cycles, final stabilization of crack opening stress values after a subsequent decay in the initially “stabilized” opening stress values is observed.

# ÖZET

ANSYS Parametrik tasarım dili (APDL) kullanılarak bir program kodu geliştirmek suretiyle, çatlak açılma gerilim değerlerini tahmin etmek üzere, yorulma çatlağı kapanmasın elastik-plastik sonlu elemanlar ile analizine kontakt elemanlar uygulanmıştır. Kontakt elemanları ile çatlak yüzeylerinin temasının ve böylece çatlak kapanmasının modellenmesi gayet doğal olmasına rağmen, kontakt elemanlarının sonlu elemanlar yöntemiyle yorulma çatlağının ilerlemesi analizlerinde kullanıldığına dair neredeyse hiç bir çalışma literatürde geçmemektedir. Geleneksel yöntem çatlak yüzeyindeki nodlara mesnet elemanları konulmasına dayanmaktadır. Rijitliği çatlağın durumuna göre ya sıfır ya da çok yüksek bir değer olarak belirlenerek çatlak yüzeylerinin teması modellenmektedir. Yük kademeli olarak uygulanırken, her kademede çatlak yüzeyindeki nodlar izlenerek açılma gerilimi tahmin edilmektedir. Bu araştırmada çatlak yüzeylerinin teması kontakt elemanları kullanılarak modellenmiştir ve bahsedilen metoda benzer bir şekilde çatlak açılma gerilimi kademeli yük uygulanması esnasında kontakt elemanlarının durumları izlenerek bulunmaktadır. İki boyutlu çatlağın ortada olduğu geometride düzlemsel birim şekil değiştirme modelinin sonlu eleman analizlerinin sonuçları literatürde belirtilen önceki çalışmalarla iyi bir uyum içindedir. Çatlak açılma gerilim değerinin her yük çeviriminde bulunması yerine, çatlak açılma gerilim değerinin sadece önceden belirlenen yük çevrim aralarında bulunmasını sağlayan bir algoritma geliştirildi. Geliştirilen algoritma ile daha az hesaplama zamanı ile, çatlak kapanması davranışının daha büyük sayıda yük çevrimi boyunca modellenmesi dağlandı. Yükün uygulanmasındaki kademe sayısının etkisi, açılma geriliminin hesaplandığı yük çevrim aralığının büyüklüğü gibi yeni parametreler incelendi. Görece daha büyük sayıda yük çevriminin simule edilmesi sayesinde açılma gerilim değerlerinin ilk "stabilizasyonundan" sonra azalarak stabilize olduğu görülebildi. Yüksek sayıda yük çevriminin simule edilme yeteneği sayesinde bu model, aşırı yüklerin yorulma çatlağının ilerlemesine etkilerinin incelenmesi için bir araç olarak kullanılabilir.

# TABLE OF CONTENTS

# LIST OF FIGURES

# LIST OF TABLES

# LIST OF SYMBOLS

| | |
|---|---|
| $a$ | Crack length |
| $h$ | Half-height |
| $E$ | Modulus of elasticity |
| $K$ | Stress intensity factor |
| $K_c$ | Critical stress intensity factor |
| $K_{th}$ | Threshold stress intensity factor |
| $K_{op}$ | Opening stress intensity factor |
| $K_{eff}$ | Effective stress intensity factor |
| $K_{max}$ | Maximum stress intensity factor |
| $K_{min}$ | Minimum stress intensity factor |
| $N$ | Number of cycles |
| $R$ | Stress ratio |
| $r_f$ | Forward plastic zone size |
| $S$ | Remote stress |
| $S_{max}$ | Maximum remote stress |
| $S_{min}$ | Minimum remote stress |
| $S_y$ | Yield stress |
| $S_{op}$ | Opening remote stress |
| $u$ | Displacement |
| $w$ | Half-width |
| | |
| $\Delta_a$ | Minimum mesh size |
| $\sigma_0$ | Flow stress |

# 1. INTRODUCTION

It has been suggested that 50 to 90 percent of all mechanical failures are due to fatigue, and the majority of these failures are unexpected. [1] Fatigue has been defined as "the progressive localized permanent structural change that occurs in a material subjected to repeated or fluctuating strains at stresses having a maximum value less that the tensile strength of the material" [2]. There are currently many approaches to fatigue design. They range from simple to complex. Initial expensive complete fatigue design, although expensive, will lower cost in the long run.

Fracture of a structural member due to repeated load is commonly referred to as a fatigue failure or fatigue fracture. The corresponding number of load cycles before fracture occurs is referred to as the fatigue life of the member. The fatigue life of a member is affected by many factors [2]. For example, it is affected by (1) the type of load (uniaxial, bending, torsion), (2) the nature of the load-displacement curve (linear, nonlinear), (3) the frequency of load repetitions or cycling, (4) the load history (cyclic loading with constant or variable amplitude), (5) the size of the member, (6) the material flaws, (7) the manufacturing method (surface roughness, notches), (8) the operating temperature (high temperature that results in creep, low temperature that results in brittleness), (9) the environmental operating conditions (corrosion) [2]. In practice, accurate estimates of fatigue life are difficult to obtain, because for many materials, small changes in these conditions may strongly affect fatigue life. Therefore testing of full-scale members under in-service conditions is needed. However, testing of full-scale members is time-consuming and costly. Therefore data from laboratory tests are often used.

Damage tolerant methodology can be used for designing initially flawed components or determining the remaining life to failure once a flaw is detected. This is particularly of interest to the aircraft industry, where cracks are commonly detected and monitored in nearly every structural component of the aircraft.

The current researches focuses on a subset of the current damage tolerant methodology, fatigue crack closure. This chapter is a brief introduction to fatigue crack closure and how it is applied to practical design. All the concepts introduced in this chapter apply to metallic materials. Numerical modeling of fatigue is an ongoing research area.

## 1.1. Fatigue Crack Propagation

If an engineering structure is subjected to repeated or cyclic loading, the structure accumulates fatigue damage. Eventually, if the cycled loads are large enough, a detectable crack will form and know the problem is to determine the remaining life of the structure, when the crack reaches a critical length where rapid fracture will occur. These cycles between crack detection and structural failure are where fatigue crack propagation takes place. Figure 1.1 shows a schematic of the regions of crack growth.

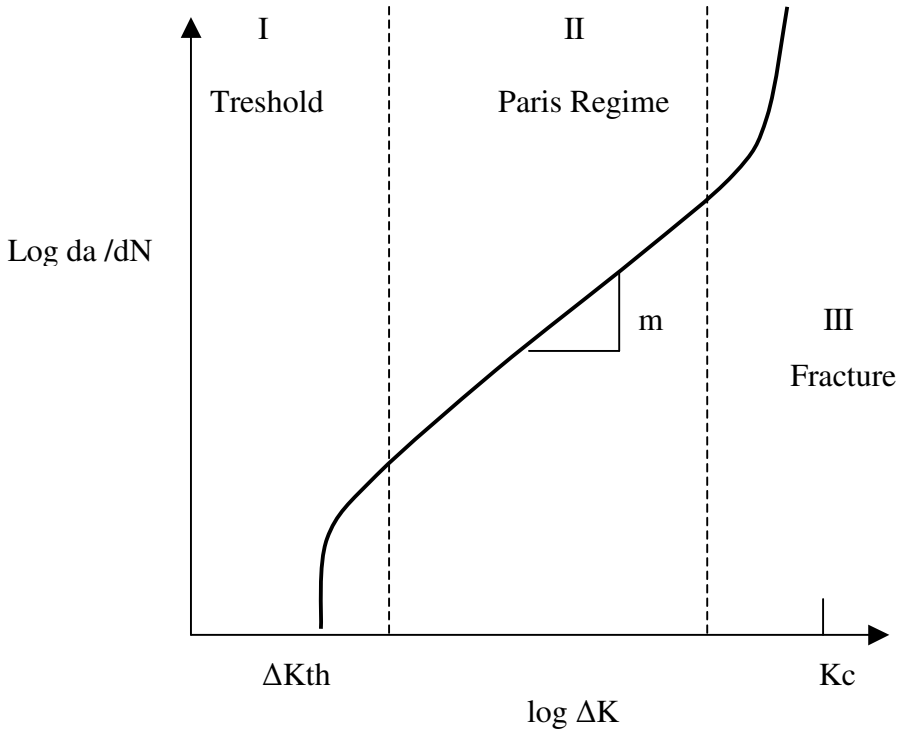


Figure 1.1. Crack Growth Behavior

This figure shows three distinct regions of crack growth. The x-axis of this plot is the difference between the stress intensity factor (which is a function of load, crack length, and geometry) at the maximum load and minimum load on logarithmic scale. The y-axis is the crack growth per cycle. Region I is the threshold regime where small changes in load (which directly affects the stress intensity factor) results in little to no detectable crack growth. Region III is the fracture regime where the maximum stress intensity factor is approaching the material dependant fracture toughness, where rapid fracture will take place. Region II is the most significant region, which has become known as the Paris regime. Crack growth is nearly linear with changes in stress intensity factor range. The well known Paris equation can be used to model crack propagation in this region:

$$da/dN = C(\Delta K)^n \qquad (1.1)$$

where C and n are material properties. For a given crack length and load level, this equation can be integrated to determine the number of cycles before the crack length reaches its critical length.

## 1.2. Fatigue Crack Closure

In 1970, Wolf Elber quantified and demonstrated the importance of a new fatigue crack growth phenomena, crack closure[3]. Based on experimental results using thin sheets of an aluminum alloy, Elber argued that a reduction in the crack tip driving force occurred as a result of residual tensile deformation left in the wake of a growing crack. Since then, several additional closure mechanisms have been identified **[**1**,** 3**-**5**],** The residual tensile deformation caused the crack surfaces to close prematurely before minimum load was reached. Figure 1.2 shows a schematic representation of the mechanisms causing fatigue crack closure [6].

In the presented research, plasticity-induced crack closure is considered. It is this type of closure that was first observed by Elber, and is caused by residual tensile deformations in the wake of a growing crack. The other closure mechanisms are often

assumed to be secondary, however multiple closure mechanisms can be present at once, increasing the closure level.

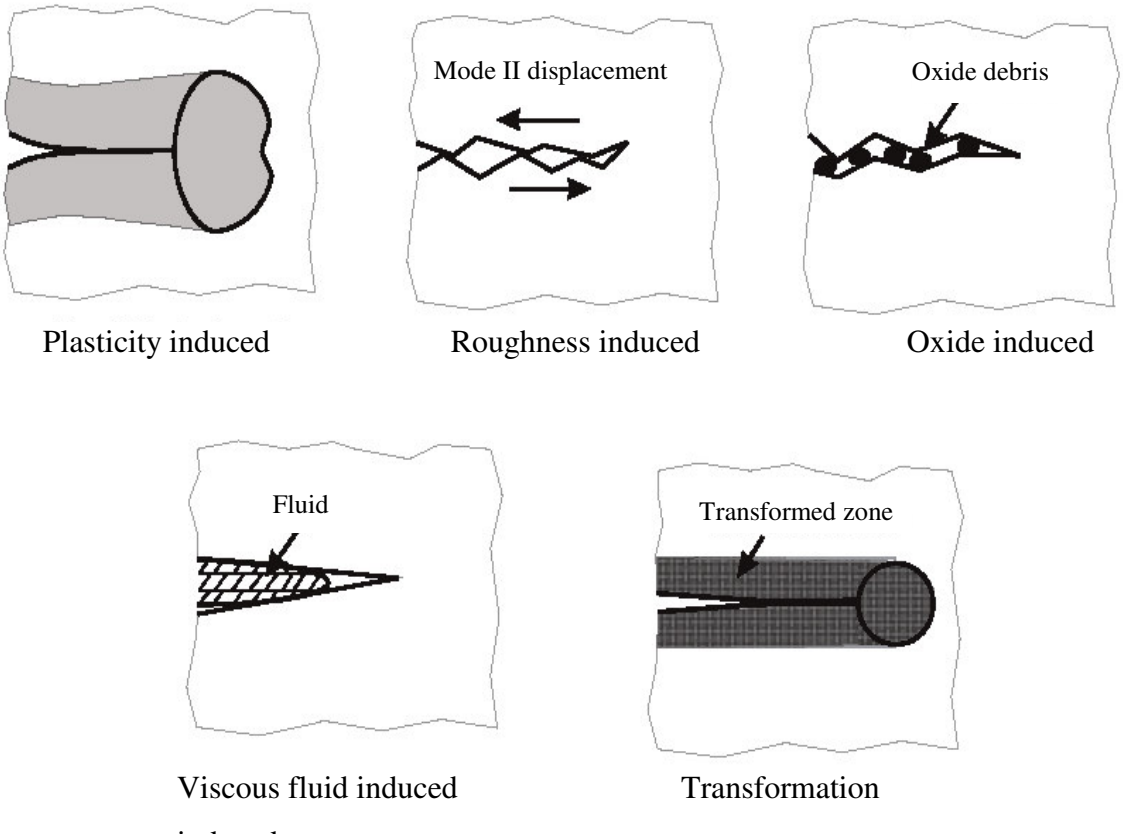


Figure 1.2. Crack Closure Mechanisms

Figure 1.3. shows the effect closure has on cyclic loading. It is assumed that no crack growth takes place during the portion of the load cycle when the crack surfaces are closed. This is implemented in the crack growth propagation equation by using a modified Paris equation that uses an effective stress intensity range to determine crack growth.

$$\frac{da}{dN} = C\left(\Delta K_{eff}\right)^m$$
$$\Delta K_{eff} = K_{\max} - K_{op} \qquad (1.2)$$

However, determination of the crack opening level is difficult. For plasticity-induced closure, approximate methods have been developed to calculate opening levels, but to ensure the accuracy of the results complex elastic-plastic finite element analyses must be performed.

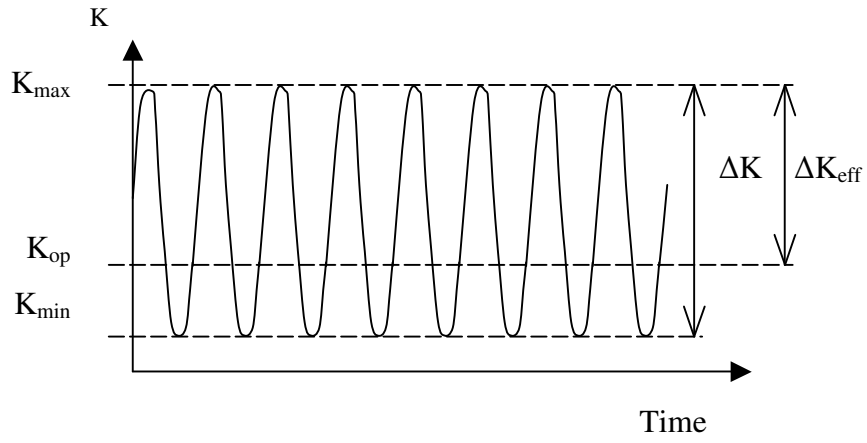


Figure 1.3 Schematic of Effective Stress Intensity Factor

The current research focuses on using elastic-plastic finite element analysis to predict plasticity-induced closure in two-dimensional geometries using contact elements, by predicting the opening stress values.

## 1.3. Crack Tip Nomenclature

As a fatigue crack propagates, two different types of crack tip plastic zones are generated as shown in Figure 1.4. The forward plastic zone is defined as the material near the crack tip undergoing plastic deformation at the maximum load. The second zone of interest is the reversed plastic zone, which is defined as the material near the crack tip undergoing compressive yielding at the minimum load. These crack tip plastic zones are used to characterize the degree of finite element mesh refinement.

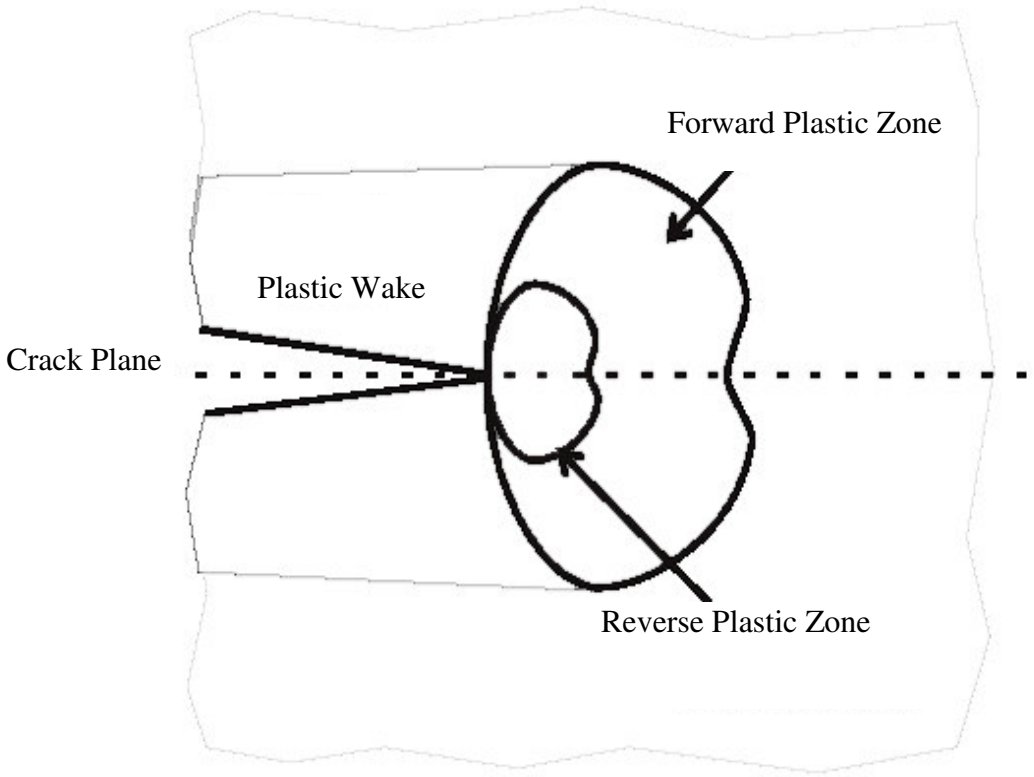


Figure 1.4. Plastic Deformation Around a Growing Crack [7]

The nature of plastic deformation near the crack tip is strongly influenced by the 2-D idealization assumed. The permanent elongation of material in the direction normal to the crack requires the transfer of material from somewhere in the cracked body due to incompressibility requirements during plastic deformation [8]. Under plane-stress, a potential mechanism of material transfer is obvious. Since out-of-plane deformation is not constrained, material can be transferred from the thickness direction to the axial direction [8]. However, the mechanism of material transfer postulated for plane-stress is not admissible for plane-strain. By definition, no net out-of-plane contraction can occur, and therefore it has been suggested that there can be no net axial stretch of material in the plastic wake behind the crack tip as discussed by Fleck [9], which implies no plasticity-induced crack closure. The existence of plasticity-induced crack closure under plane-strain conditions has been a topic of intense debate [10-20].

Many researchers have performed finite element analyses simulating plasticity-induced fatigue crack closure, considering different two-dimensional configurations under plane-strain or plane-stress conditions [8-35]. Far fewer efforts have been directed toward the three-dimensional problem [7,35-42]. Newman [30] has presented general reviews in his papers. A comprehensive parametric analysis is carried out by Solanki [23].

In this research work, finite element analysis of plasticity-induced fatigue crack closure for two dimensional plane strain geometries is performed. Emphasis is focused on the using contact elements to model crack closure and to opening stress value.

# 2. LITERATURE REVIEW

A number of researchers have attempted modeling plasticity-induced crack closure using the finite element method. While some researchers have attempted three-dimensional models, the majority of the finite element analyses performed model crack closure in two-dimensional geometries. While simplistic in nature, the results from the two-dimensional analyses are important because they give insight into some of the more common modeling issues related to crack closure. The basic algorithm employed by all the studies investigated is the same. A mesh is created with a suitably refined region near the crack front. An elastic-plastic material model is employed so plastic deformations occur in the vicinity of the crack tip. Remote tractions are then applied to the model and cycled between a maximum nominal stress $S_{max}$ and a minimum nominal stress $S_{min}$. During the load cycle, the crack front nodes are released, advancing the crack one elemental length da, which allows for the formation of a plastic wake. Stresses and displacements for the crack surface nodes are monitored to detect contact between crack faces, and thus predict crack closure. This process is repeated for several load cycles until the crack opening stress values stabilize. Figure 2.1 is a descriptive sketch of the algorithm. Skinner[7] replaced the truss elements used by Newman [30] with fixed boundary conditions. Although the algorithm is simple, the problem of modeling contact, at which stage the crack is to be advanced, and how the crack opening is assessed is treated differently by various researchers. These different approaches and the research on the effects of the parameters like material model, mesh refinement are reviewed in this chapter.

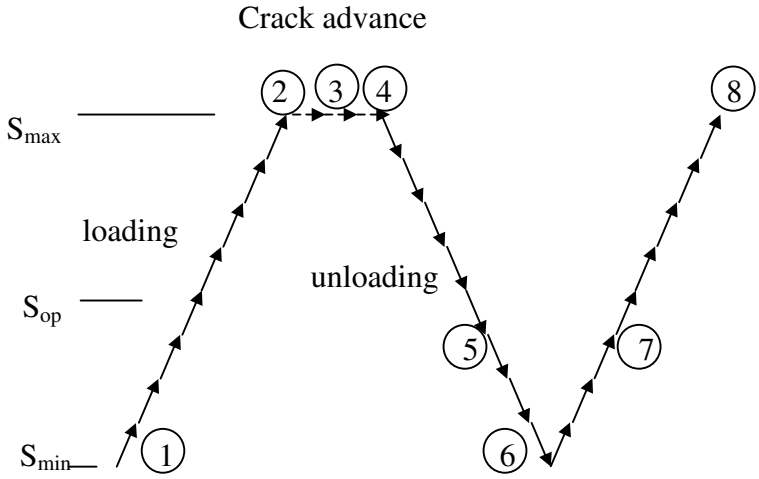


1. Initial state at minimum load
(dashed line shows the initial crack tip)

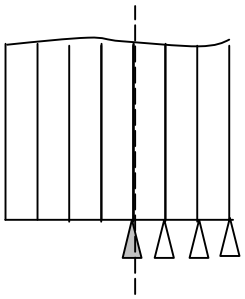

2. State at maximum load

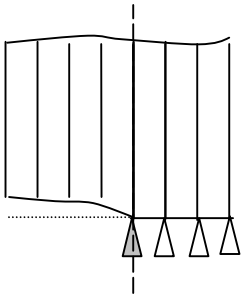

3. and 4. Incremental crack advance by replacing the boundary condition at the crack tip with a fraction of the reaction force developed at the crack tip node and incrementally decreasing to zero.

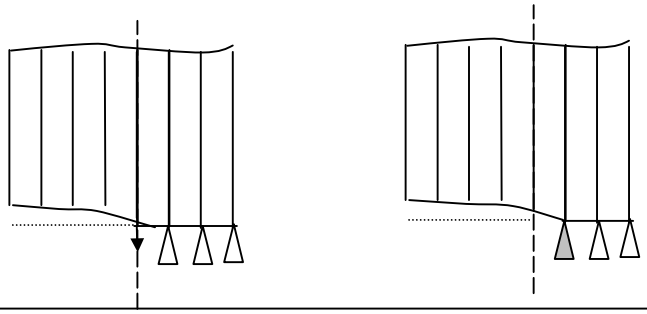

Figure 2.1. Descriptive sketch of the crack closure model.(continues)

5. During incremental unloading some of the nodes at the crack surface begin to penetrate. At every load level the nodes which are detected as penetrating are fixed.

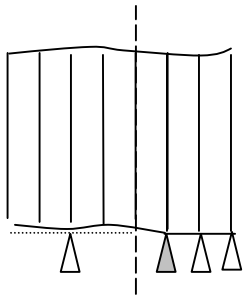

6. At minimum load

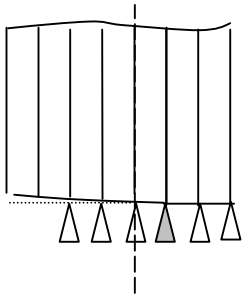

7. During incremental loading the nodes at which nodal reaction force becomes positive the nodal fixity is removed, the node tends to open. If the last node looses contact, crack opening stress is calculated by interpolation based on the reaction forces at the current and previous –unopened- load level.

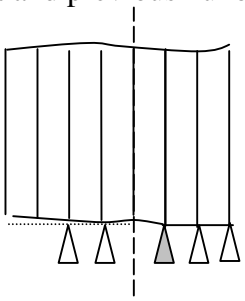

8. At maximum load

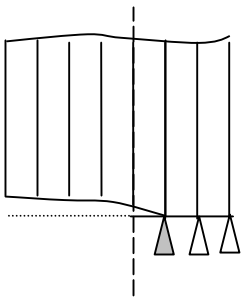

Figure 2.1. (continued) Descriptive sketch of the crack closure model.

## 2.1. Crack Surface Contact

A changing boundary condition characterizes a crack under cyclic loading. To prevent the crack surfaces from penetrating as the minimum load is approached, some mechanism must be implemented into the finite element simulation.

This can be achieved by changing the stiffness of spring elements attached to the crack surface, by removing or imposing crack surface nodal constraints, by using truss elements on the crack surface, or by using contact elements. The implementation of contact elements along the crack surface, however, is not been done yet, because it can lead to convergence problems and long execution times [7]. Newman [30] was the first to implement spring (truss) elements to simulate the changing boundary condition. The element was connected to each boundary node on the crack surface. For open nodes, the spring stiffness was set equal to zero, and for closed nodes, the stiffness was assigned a large value. McClung et al. [8, 24, 25, 28, 29, 33, 34] followed Newman's approach in their earlier studies. However, the large imposed stiffness values for constrained crack surface nodes were found to be a source of numerical difficulties, and they investigated an alternate approach to simulate the cyclic crack surface contact. During loading and unloading, stresses and displacements were monitored along the crack surface. A negative nodal displacement indicated that the crack was closed at this point, and the displacement was set to zero. A tensile nodal stress indicated that the crack was open at this point, and the nodal restraint was removed. This more direct approach has also been used by Blom et al. [11]. Wu et al. [31] have used a truss element with a varying stiffness together with pairs of contact elements and the element death option. The element death option was incorporated to deactivate truss elements or cut the truss elements. They have shown that with this approach a node can be released any time during a load cycle irrespective of the magnitude of the deformation caused by the release of the node. Consequently, fewer problems with convergence were encountered and also several nodes can be released simultaneously.

## 2.2. Mesh Refinement

As a fatigue crack propagates, two different types of crack tip plastic zones are generated. The forward plastic zone is defined as the material near the crack tip undergoing plastic deformation at the maximum load. The second zone of interest is the reversed plastic zone, which is defined as the material near the crack tip undergoing compressive yielding at the minimum load [5]. These crack tip plastic zones have been used to characterize the degree of finite element mesh refinement required when modeling plasticity-induced closure [13, 21, 22].

Newman [30] was the first to study the effects of finite element mesh refinement on opening load computations under plane-stress conditions. He modeled a center crack specimen of width 2W with constant-strain triangle (CST) elements and found that the crack opening loads converged with increasing levels of mesh refinement at high applied stress levels as shown in Figure 2.2.

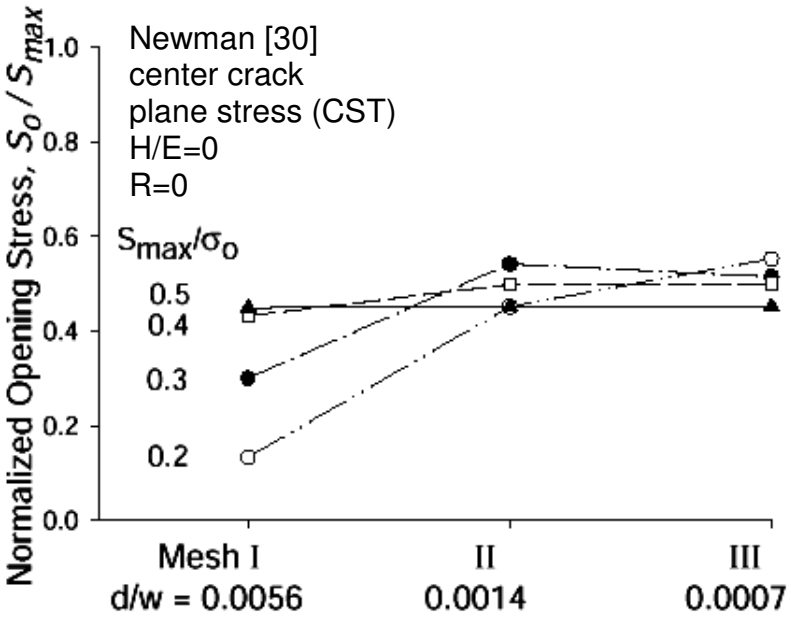


Figure 2.2 Mesh Refinement Studies

In the figure, d is the element size ahead of the crack tip. For small applied stresses, convergence was not observed. Convergence may be a consequence of the number of elements present in the reversed crack tip plastic zone. Newman considered the discretization of the forward plastic zone only, and did not consider the reversed plastic zone. Thus, the reversed zone may have been discretized with an insufficient number of elements.

McClung et al. [8, 24, 25] performed mesh refinement studies on a crack emanating from a circular hole, the center crack specimen, and an edge-crack specimen. They found that mesh refinement should be based on the number of elements present in the forward plastic zone in the crack plane. They also suggested that adequate refinement to capture the reversed plastic zone may be important. Dougherty et al. [13] performed mesh refinement and element shape studies on compact tension and center crack geometries under plane-strain, and found that an aspect ratio less than or equal to 2 should be used for elements ahead of the crack. They also found that the mesh density ahead of the crack should satisfy $\Delta a/r_f \leq 0.1$, where $2r_f$ is an approximation of the forward plastic zone given by:

$$r_f = \frac{1}{2\alpha\pi}\left(\frac{K_{\max}}{\sigma_0}\right)^2 \tag{2.1}$$

where $\alpha$ is equal to 1 and 3 for plane-stress and plane-strain respectively, $\sigma_o$ is the flow stress, and $K_{max}$ is the maximum stress intensity factor. Park et al. [32] suggested that mesh refinement levels for the center crack specimen should be chosen to produce opening stress values that compare well with experimental results. In the opinion of the authors, this approach is flawed given the difficulties associated with measuring opening load values [36, 43-46].

Most of the work reported in the literature has incorporated large applied stresses, which allows for the use of coarse meshes while still satisfying mesh refinement requirements.

## 2.3. Stabilization of Crack Opening Load

Under constant amplitude loading, the crack opening load will typically increase monotonically with increasing crack growth until a stabilized value is reached as illustrated in Figures 2.3 a and 2.3 b

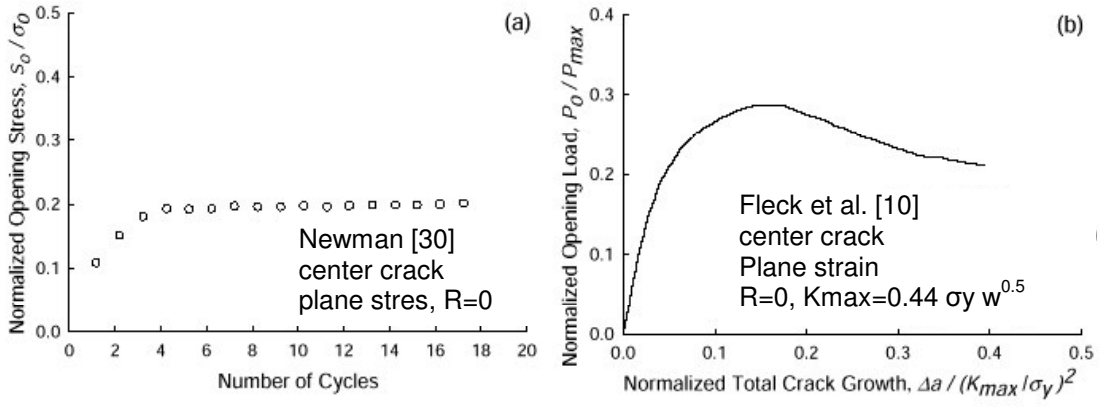


Figure 2.3. Stabilization of Crack Opening Values under Plane-stress and Plane-strain

McClung [8] has shown that under constant amplitude loading conditions, the crack must be advanced completely through the initial forward plastic zone to form a stabilized plastic wake. This is necessary to obtain non-varying crack opening values. However, Fleck et al. [10] and Wu et al. [31] have shown a variation in crack opening values even after the crack has progressed through initial forward plastic zone. Fleck's results are shown in Figure 2.3 b. Using a strip-yield model, Daniewicz et al. [47] have shown that a large amount of crack growth will produce a decreasing opening value if the remaining ligament becomes small enough. Achieving the large amounts of crack growth required to observe an initial stabilization followed by a subsequent decay in the crack opening value is difficult when using finite element analysis, because of the computationally intensive nature of the simulation. However, such an effort has been reported by McClung [33]. Recently Lee and Song [48] reported to obtain a stabilized crack opening level for plane strain conditions, the crack must be advanced through approximately four times the initial monotonic plastic zone.

## 2.4. Crack Advance Scheme

To produce a plastic wake behind the crack tip, the crack must be incrementally advanced in some fashion under the applied cyclic loading. The most common means of crack advance is to release the crack tip node, thus advancing the crack by an amount equal to the crack tip element size. It is important to realize that modeling an incremental crack advance with a node release involves no consideration of the physics of fatigue crack growth, since the crack extension is independent of stress level and the strain in the vicinity of the crack tip. Consequently, the finite element analysis is used to predict the crack opening value, but not the fatigue crack propagation life. Recently, some researchers have suggested the use of a cohesive element to advance the crack in a physics-based manner [49]. Newman used a critical strain to advance the crack [30].

When performing analyses using the conventional node release technique, the preferred node release scheme for simulating an incremental crack advance is unclear. The crack tip node may be advanced at the minimum load level [8, 21, 26, 27, 31, 52], at the maximum load level [9, 11, 14, 16, 28, 32-33], after the maximum load [20, 24, 25] or during the loading/unloading cycle [8, 26].

Advancing the crack at the maximum load level may create convergence problems; conversely, there is no such problem with advancing the crack using the minimum load level scheme. The convergence problem related to the maximum load release can be eased by incrementally releasing the crack front nodes [11, 21]. Some research [8, 21] has concluded that in terms of the resulting crack opening value, there is no difference when using the either maximum or minimum load node release schemes. However, other research has shown significant differences [ 24, 25, 31].

Figure 2.4 a shows results from a crack advance scheme comparison performed by McClung et al. [24, 25]. From the figure, there is a significant difference in opening value when using a different crack advance scheme. Later, McClung et al. [8] showed that this difference was a consequence of using truss elements for crack surface node fixity, and that changing the boundary conditions on the crack surface nodes directly yields

approximately the same results for the different crack advance schemes. Wu et al. [31] in their independent study found a variation in crack opening values when using the minimum and maximum loading node release schemes, and their results are shown in Figure 2.4 b. This difference may be a consequence of computing the crack opening values based upon zero crack tip nodal reaction force, which is likely influenced by the size of the elements near the crack tip. This variation may also be due to a insufficient discretization of the reversed plastic zone.

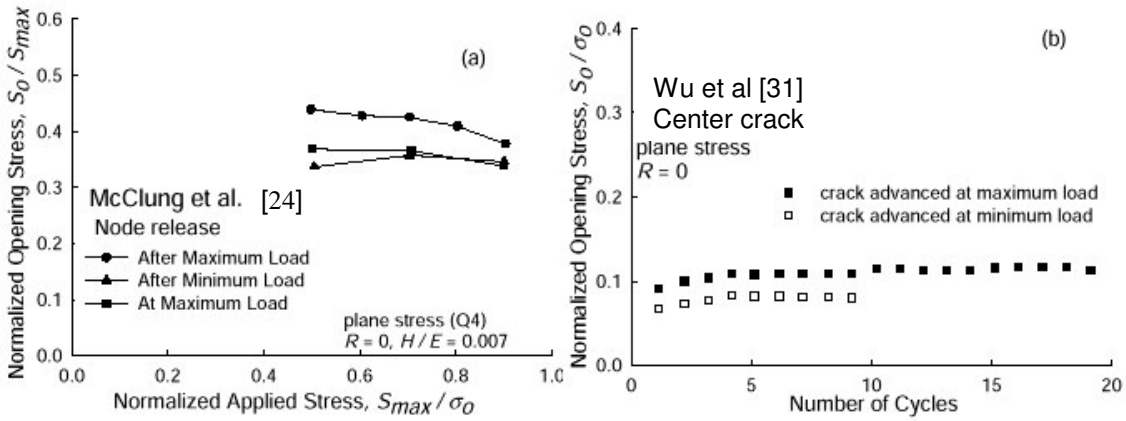


Figure 2.4. Comparison of Crack Opening Values Based on Crack Advance Scheme

## 2.5. Crack Opening Assessment Location

Under constant amplitude loading, the crack tip is the last point to open along the crack surface under an increasing load. Most researchers have used the first node behind the crack tip to assess the crack opening values [8-12, 14-35]. Wu et al. [31] have used the crack tip itself to assess the crack opening values. They have proposed that when the compressive stress borne by the crack tip node changes to a tensile one, the crack is fully open. Others have used the second node behind the crack tip [22, 8]. McClung et al. [8] and Fleck et al. [9] have shown that the results obtained when using first node behind the crack tip can be mesh dependent.

## 2.6. Plane-stress and Plane-strain Condition

The nature of plastic deformation near the crack tip is strongly influenced by the two-dimensional idealization assumed. The permanent elongation of material in the direction normal to the crack requires the transfer of material from somewhere in the cracked body due to incompressibility requirements during plastic deformation. Under plane-stress, a potential mechanism of material transfer is obvious. Since out-of-plane deformation is not constrained, material can be transferred from the thickness direction to the axial direction. However, the mechanism of material transfer postulated for plane-stress is not admissible for plane-strain. By definition, no net out-of-plane contraction can occur, and therefore it has been suggested that there can be no net axial stretch of material in the plastic wake behind the crack tip, which implies no plasticity-induced crack closure [8-9,13, 21]. The existence of plasticity-induced crack closure under plane-strain conditions has been a topic of intense debate [10- 20].

A study of crack tip plastic zone sizes and crack opening behavior for the center crack specimen under plane-strain and plane-stress conditions has been performed by McClung et al. [24, 25]. Crack closure was found to occur in plane-strain, with lower opening values than those observed under plane-stress.

A combined numerical and experimental study of crack closure in AA2024-T3 was conducted by Blom and Holm [11]. A plane-stress and plane-strain model of the compact tension specimen was constructed with constant strain triangular (CST) elements. Under plane-strain conditions closure was observed, and the plane-strain closure levels were smaller than those for plane-stress.

Their results are also questionable due to a relatively coarse mesh. Under a stress ratio R = -1, Lalor and Sehitoglu found that the plane-strain closure levels were lower than those for plane-stress. However, when the applied stress was increased to $S_{max} / \sigma_o = 0.8$, the opening values were larger [20].

Dougherty et al. [13] performed two-dimensional analyses of compact tension and center crack geometries under plane-strain, and demonstrated a good comparison between predicted closure levels and experimental results. Their finite element meshes were composed of four-noded and eight-noded quadrilateral elements. Ashbaugh et al. [12] performed a study similar to that conducted by Blom and Holm [11], focusing on finite element analysis of plasticity-induced crack closure in the compact tension specimen under plane-strain conditions. In their analyses four-noded quadrilateral elements were used, and their results indicated that closure does occur in plane-strain. Again, their results are also suspect due to a lack of mesh refinement and potential plane-strain locking. Conversely, Fleck and Newman [10] have shown that closure does not occur for a bend specimen under plane-strain conditions, while closure does occur for the center crack geometry under plane-strain.

## 2.7. Constitutive Model

Most researchers assume a material that is elastic-perfectly plastic. However, some research has been performed to determine the effect of material hardening. A significant change in opening behavior was found when different hardening slopes where assumed. For low loads ($S_{max} / \sigma_0 < 0.6$) a higher hardening modulus resulted in lower opening levels [35].

## 2.8. Overview

In this thesis, contact elements are implemented into the elastic plastic finite element analysis of plasticity-induced fatigue crack closure by developing a code using ANSYS Parametric Design Language(APDL). Two dimensional plane strain analyses finite element analyses are carried out for the center cracked geometry. Rather than determining crack opening stress of every load cycle, an algorithm that makes it possible to find crack opening stress at predetermined load cycle intervals is developed. With the developed

algorithm it was possible to analyze crack closure behavior during a larger number of load cycles with less execution time. The newly introduced parameters such as effect of the number increments of the applied load, the effect of the load cycle interval where the opening stress values are determined are investigated.

# 3. FINITE ELEMENT MODEL

The plasticity-induced crack closure model concepts were incorporated into the finite element package ANSYS using Parametric Design Language (APDL) by Skinner[7]. Analyses are carried out using ANSYS version 5.4 [53]. The model of Skinner is modified to implement contact elements in the prediction of plasticity induced fatigue crack closure. Moreover a routine is developed to determine the crack opening stresses at predetermined load cycle intervals, which enables to increase the total number of simulated fatigue cycles without increasing the execution time. The code used in the analyses is listed in the Appendix.

The approach is actually simple, a finite element mesh is generated, the crack is modeled in the mesh, appropriate symmetry boundary conditions are applied, loading is done in cycles alternating between maximum stress and minimum stress. After maximum stress is applied the crack is advanced by one element size, da. At the predetermined load cycles the crack opening stress is determined with the developed routine within the "resolution" of 1/100 of the maximum stress by incrementally applying the load in 100 load increments.

## 3.1. Finite Element Model Basics

A two dimensional plane strain model is created with half-width w=230 mm, half height h=460mm and crack length a= 0.0279mm. Due to symmetry only one fourth of the specimen is modeled. The modeled section is shaded in Figure 3.1. This specimen is first modeled by Newman [28] and than by Skinner [7].


Figure 3.1. Geometry of the model

The boundary conditions and the loading is schematically shown in Figure 3.2. At x=0 all the nodes are fixed in the x direction to model symmetry at y-axis. Similarly the nodes at y=0 except the ones on the crack surface are fixed, to model vertical symmetry. At the top surface of the geometry, the loads are applied as the corresponding pressure values.

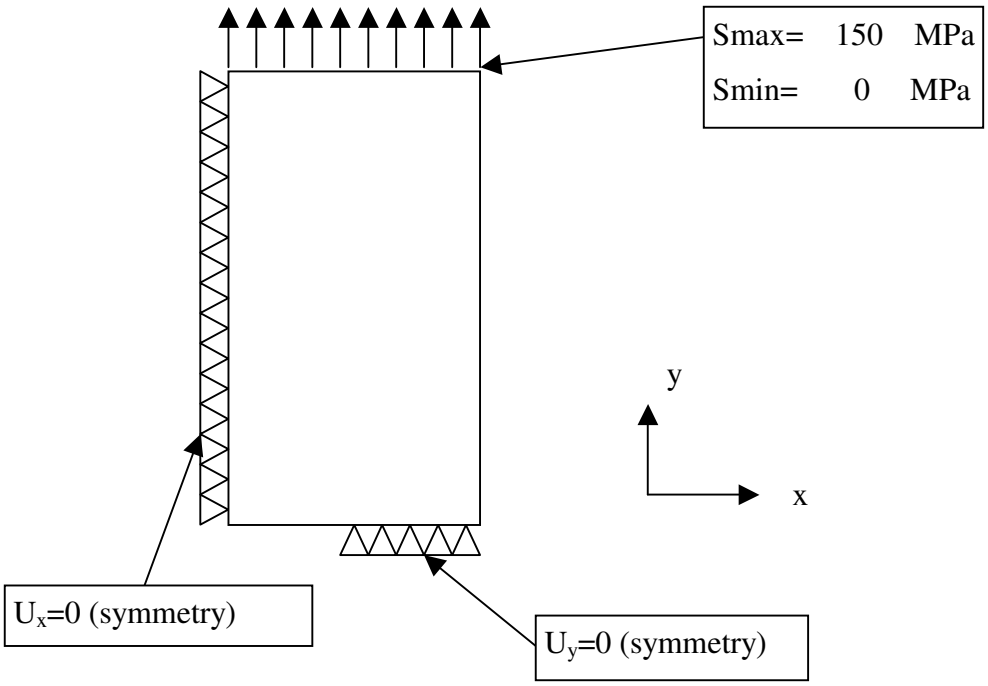


Figure 3.2. Schematics of the boundary conditions and loading.

Non-linear material properties must be used to model plasticity-induced closure. For simplicity, an elastic perfectly plastic material is assumed (Figure 3.3.) is used for all the models in the present study. The modulus of elasticity E is 70000MPa, and yielding stress $\sigma_o$ is 350 MPa. The surface traction applied to the top surface of the model is cycled between Smax= 150 Mpa and Smin=0 Mpa.

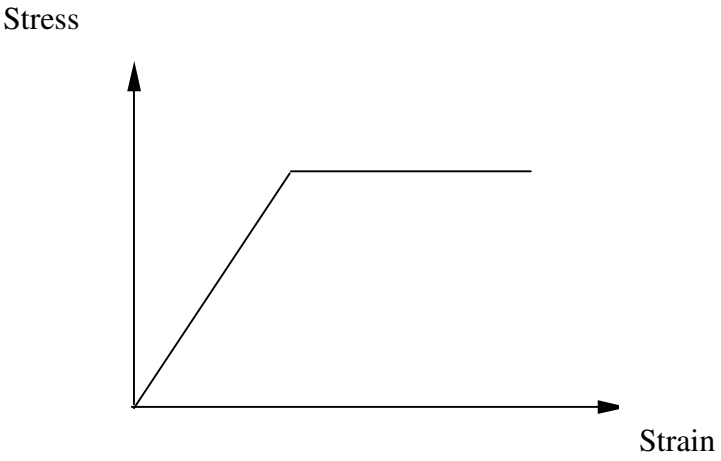


Figure 3.3. Elastic-perfectly plastic material model.

The crack growth increment, da = 0.18 mm is equivalent to the mesh used by Newman for the same geometry. However, the mesh used by Newman was composed entirely of three noded triangular elements. In the current analyses, linear four nodded solid elements are used for two-dimensional analyses. The mesh used in this work is shown in Figue 3.4. These elements are designated as PLANE42 in ANSYS. Since linear elements are used, care must be taken to ensure that poor element aspect ratios (ratio of longest edge to shortest edge) are not compromising results. Long slender elements in areas of near constant stress should not affect the results. However, in areas of large strain gradients (i.e. the crack tip) the element aspect ratios should be as close to unity as possible.

To model the contact, point to surface contact elements are used. They are designated as CONTAC26 in ANSYS. Contact elements are generated for the nodes on the carck surface and for nodes which will be released during crack advance. The symmetry plane is defined as the contact surface, which is rigid and fixed by default, if CONTAC26 elements are used.

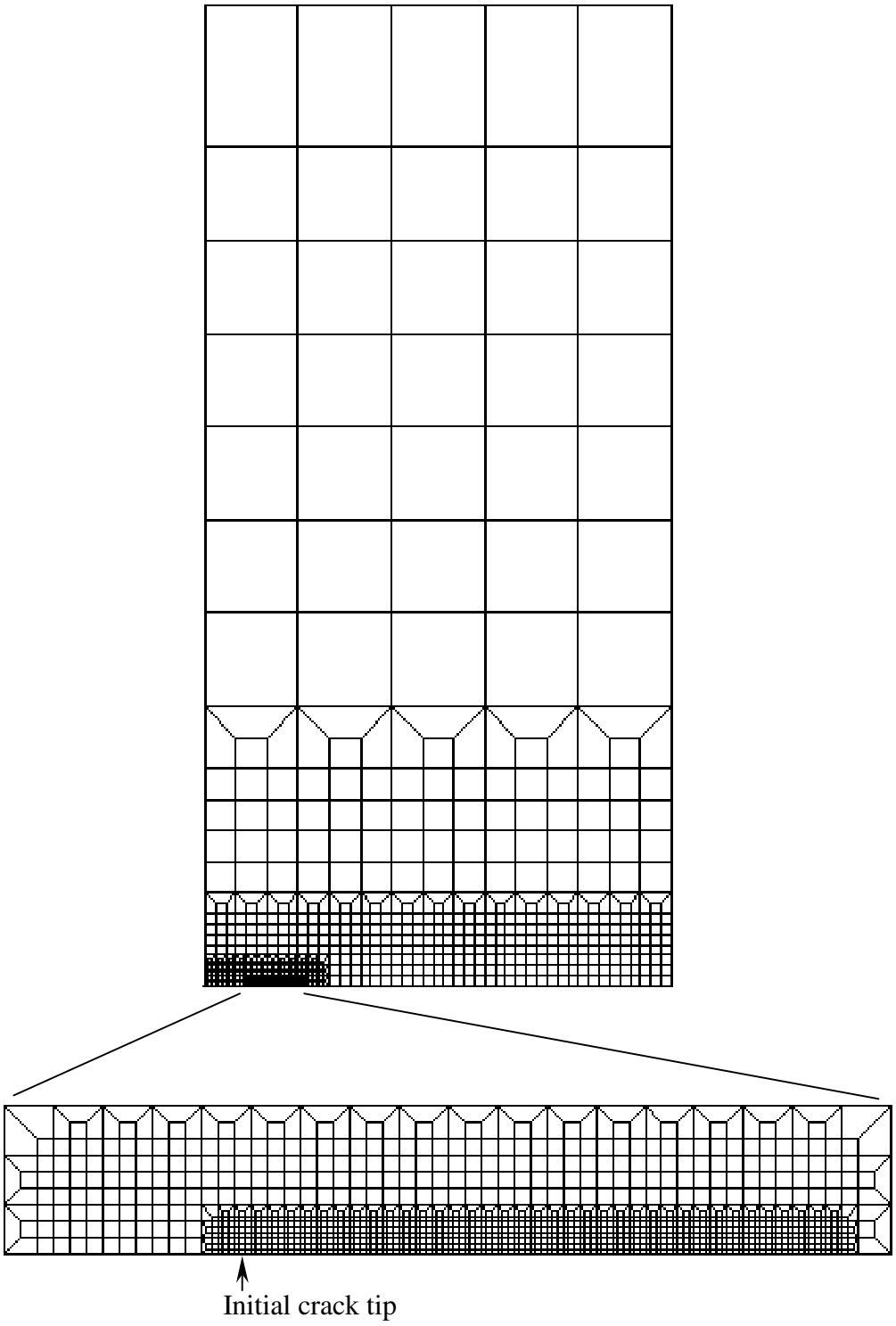


Figure 3.4. Finite element mesh

Adequate mesh refinement is always an issue when conducting finite element analyses. The idea is to have enough refinement to capture all strain gradients of interest, but to avoid excess refinement, which can lead to unnecessarily long run-times. For two-dimensional plane-strain closure analyses when R = 0, it has been suggested that the mesh should be refined such that there are approximately ten elements contained in the forward plastic zone [35]. Also, it has been observed that for crack opening level stabilization to take place, the crack must be advanced completely through the initial forward plastic zone [35]. The mesh size criteria $\Delta a/r_f \leq 0.1$ is used. Forward plastic zone size, $r_{f,}$ is calculated by McClung and Sehitoglu [50, 51]as follows:

$$\frac{r_f}{a} = \left( \frac{S_{\max}}{\sigma_0} \right)^2 \tag{3.1}$$

where,

$r_f$ = crack forward plastic zone size

$S_{max}$ = maximum stress

$\sigma_0$ = material yield stress

### 3.2. Crack Closure Model

The crack is modeled by fixing the nodes at the uncracked region in y-direction. The nodes at the crack surface are left.

Modeling of plasticity-induced fatigue crack closure is actually the modeling the formation of a plastic wake. This formation of a plastic wake can be simulated by advancing the crack tip through the initial monotonic plastic zone. In reality, crack advance takes place in very small increments over several cycles. Unfortunately, the finite element requires this crack advance to be discretized and to take place at a specific load. When using the finite element method crack growth can take place only in integer multiples of the element length, da, at the crack tip.[ 7]. It should be recalled that the finite element

analysis is used to predict the crack opening value, but not the fatigue crack propagation life.

A more complicated problem is that, at what point during the load cycle should crack advance take place. Many researchers suggest crack advance should take place at the minimum load to aid in convergence [28]. Other researchers, however, suggest that crack advance at minimum load is physically unrealistic, since in reality there are no mechanisms present to cause crack growth on a closed crack. Instead, they suggest that crack advance should take place at the maximum load [30]. In the present study, crack advance occurs at the maximum load, but to ease convergence the crack front nodes are released incrementally, as was suggested by Skinner [7]. This is accomplished by determining the crack front reaction forces present at maximum load. The crack front fixities are then removed, and are replaced with a force that is a fraction of the reaction force. The force is then gradually removed until it can be totally removed without convergence problems.

In the present work, the crack advanced scheme of Skinner [7] is used and the reaction force is bisected four times before being removed completely. Also, it should be noted that crack advance is uniform with each point on the crack front moving forward one element width perpendicular to the crack front. Consequently, crack aspect ratios are fixed throughout the crack growth process.

### 3.3. Modeling of the Crack Surface Contact

In order to prevent the crack surfaces from penetrating, some mechanism must be implemented in the finite element script. In spite of the fact that the use of contact elements in modeling crack surface contact, and thus in modeling of crack closure is inherently natural, almost no effort to incorporate it in the finite element analysis of fatigue crack growth has been reported in the literature.

The most commonly used method, which was first used by Newman [28] and modified by Skinner[7] and Solanki[23] will be shortly reviewed here, because the results of this study will be compared with their results.

The loading and unloading is applied incrementally. At each load increment the crack surface node displacements are monitored. The original method proposed by Newman[28] is as follows: Once they become negative, a very large stiffness is added to the diagonal of the assembled finite element stiffness matrix, which prevents further penetration. This "spring" is removed when the crack surface begins to open again on the subsequent loading. Skinner modified this method to adapt to the commercial Finite Element Analysis Package ANSYS [7]. The following scheme was used. During loading and unloading, the remote loads are changed by small load increments. At the end of each load increment, the status of each of the crack surface nodes is checked. During unloading, the displacement of each node is monitored. If the displacement becomes negative, a nodal fixity is immediately applied preventing the node from further penetration. On the subsequent loading, the reaction forces on all of the nodes on the crack surface that closed are monitored. If the reaction forces on the nodes become positive (the node is in tension), the nodal fixity is removed. The remote load at which the last nodal fixity is removed is the crack opening load. Unfortunately, the opening load can be found only to the resolution of the loading increment[7].

To obtain a better estimate of the load when the crack surface actually opens, linear interpolation was used. For, the load step before the crack surface node opens, the nodal reaction force is negative. Upon opening, the reaction force becomes positive. Linear interpolation is used to determine the remote load at which the reaction force became zero (Figure 3.5.). This is what is reported as the opening load for that specific node.[7]

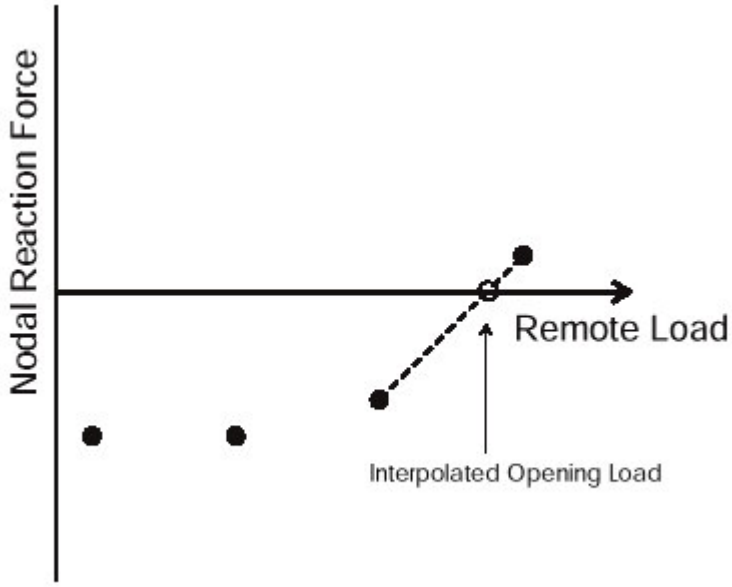


Figure 3.5. Interpolation for Node Opening Load[7]

The closure model of Skinner is graphically summarized in Figure 3.6. Initially a large load increment is used to save execution time. After the first node on the crack surface opens, a smaller load increment is used until all the nodes on the crack surface is open. A larger load increment is then used until the maximum load is reached, at which point crack advance takes place. The first load step of crack advance, the nodal fixities on the crack front are removed and are replaced by a force equal to 50 per cent of the node reaction forces. The forces are then reduced over three additional load steps when they become near zero, after which they are completely removed. The entire crack front has now advanced one elemental length perpendicular to the crack front. Unloading then takes place. Similar to the loading, a large increment is used initially, which is decreased when the crack begins to close and is increased again after the entire crack surface has closed. These load cycles are repeated several times until the crack opening levels reach stabilized values. [7]

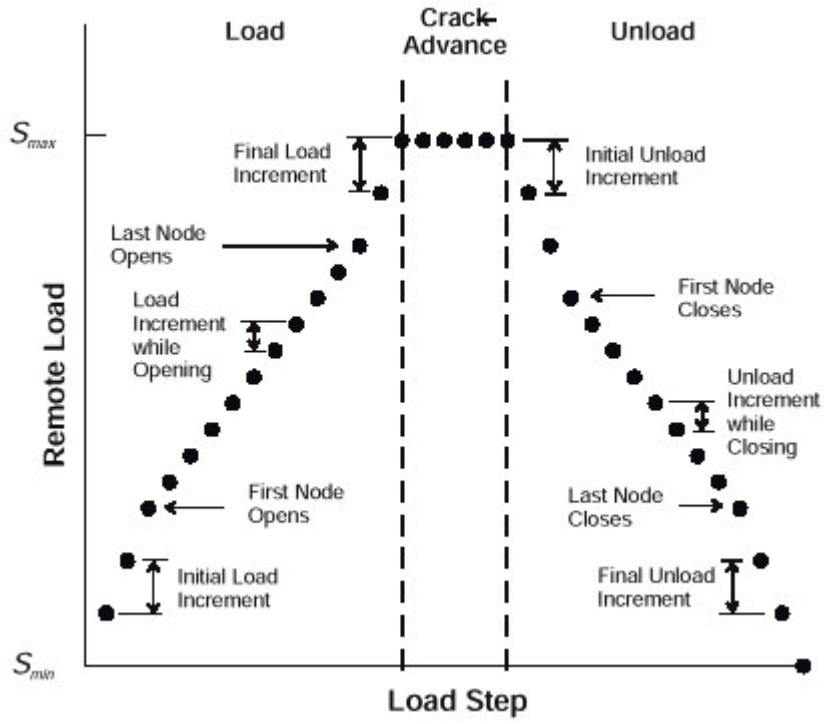


Figure 3.6 Typical Load Cycle [7]

The implementation of the contact elements into the finite element analysis of fatigue crack closure is accomplished by following algorithm. Figure 3.7. shows schematically for a representative crack opening value how the crack opening value is determined. Similar to the previous model explained above the load is applied incrementally. The application of the load is divided -as a result- into 100 increments. This is done iteratively: First the maximum load is divided into 5 increments and these load increments are applied subsequently. At the end of each load increment the status of the contact elements is monitored. For a contact element the normal for is equal to zero if the node and the surface are not in contact, otherwise the contact element normal force has a stress value in order to prevent penetration of the node into the contact surface. If the total normal force of all the contact elements is zero, the crack is open. If at the end of the load increment the sum of the normal forces is not equal to zero the next load increment is applied. If the sum of the normal forces is zero then the next iteration starts form the unopened state, which was saved previously. The next iteration of load increments is carried out in the interval and is divided into 5 increments. If inside this iteration the crack opening is detected, next load

increment iteration is started where the number of increments is 4 and the analysis is retarted from the previously saved state. The overall effect of this load increment iteration yields 5 x 5 x 4 = 100 increments. That can be called as the “resolution” of load increments. If the last interval is reached crack opening value is calculated as the average of the load levels of the last interval. One can note that the load incrementation stops if the crack opening is detected at every load increment iteration. Skinner used a resolution of 20 [7].

The next algorithm developed in the current research is a routine to determine the crack opening stresses at predetermined load cycle intervals, which enables to increase the total number of simulated fatigue cycles without increasing the execution time. Figure 3.8. schematically presents how the routine for the determination crack opening stress ($S_{op}$) value is incorporated in to the load cycles. The maximum and minimum loads are applied in cycles, and at every maximum load the crack is advanced by the mesh size at the crack tip ,da, without determining the crack opening stress value. If the start of the predetermined load cycle is reached, the current state of the analysis is recorded for later restart. From this point on the routine for the determination crack opening stress value is executed and the crack opening values is found. With the determination of the crack opening value the routine stops, records the value and the saved state at the beginning of the load cycle is recovered. From this point on the application of load cycles continues without determining the crack opening values until the next predetermined load cycle number is reached. This routine reduces the execution time appreciable for the same number of cycles if the predetermined load cycle interval is big. If the predetermined load cycle interval is one, which means that crack opening value is determined at every load cycle, the execution time is comparable with the previous method in the literature with a slight decrease in execution time.

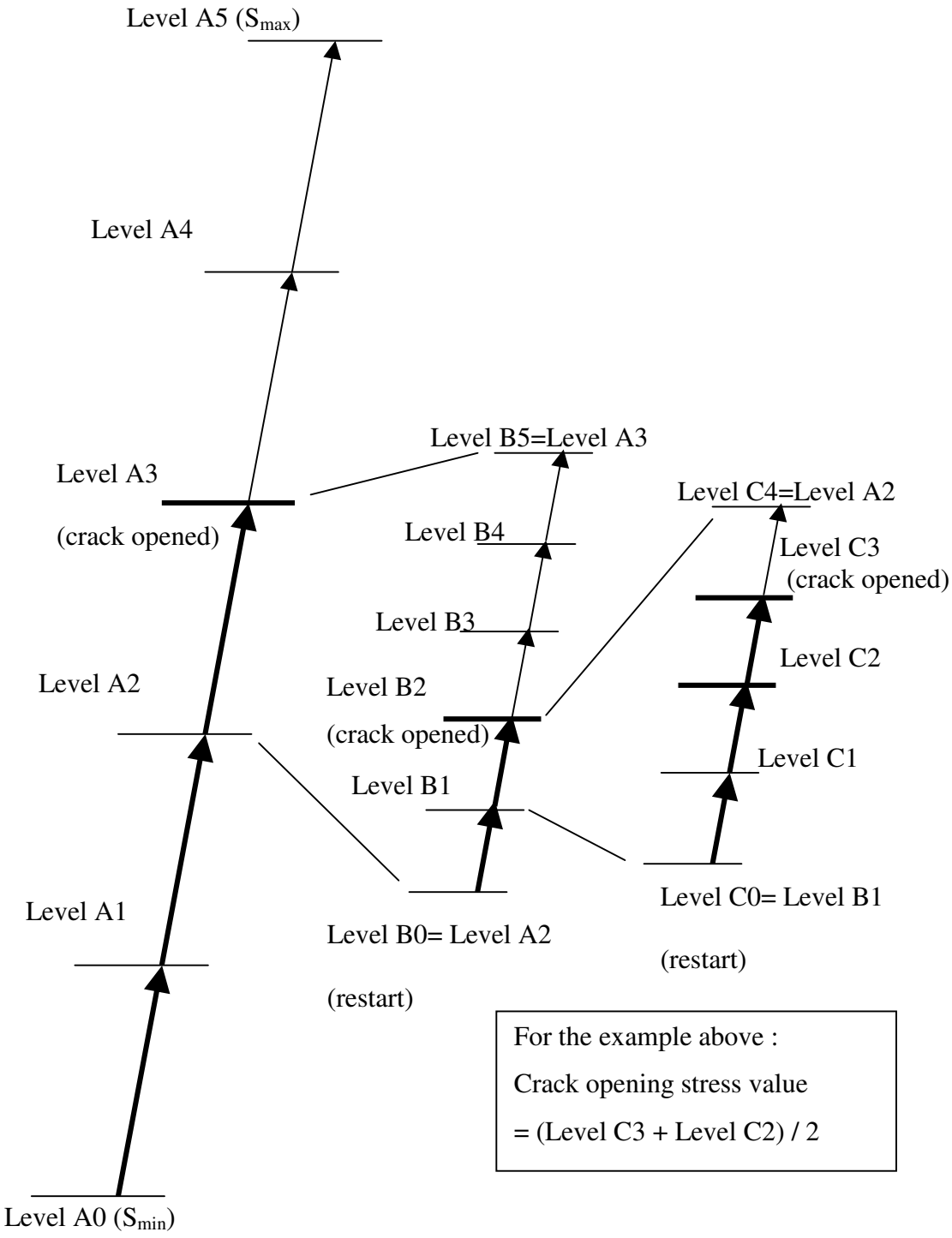


Figure 3.7. Schematic presentation of the determination of opening stress during loading for a representative opening stress value. In this figure the detected value is ($S_{max}$-$S_{min}$) 47/100. The load steps after crack is fully open are not executed, and are shown with thin arrows in the figure.

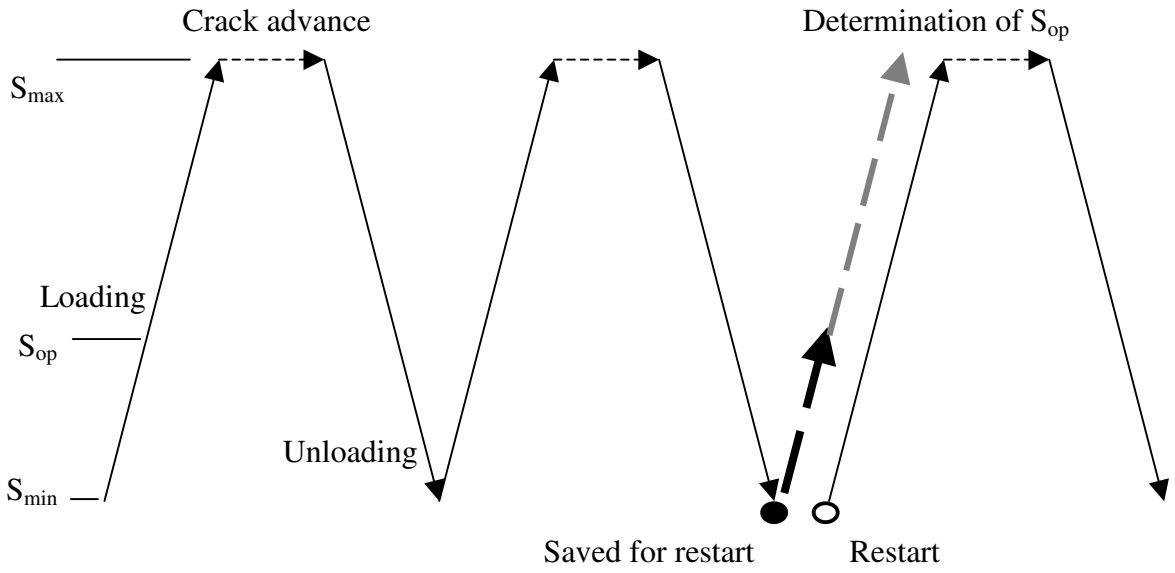


Figure 3.8. Schematical presentaion of how the routine for the determination crack opening stress ($S_{op}$) value is incorporated in to the load cycles.

With the combination of the two algorithms more cycles could be simulated. Fleck et al. [10] and Wu et al. [31] have shown a variation in crack opening values even after the crack has progressed through initial forward plastic zone. Fleck's results (Figure 2-2b) are showed a final stabilization after an initial stabilization followed by a subsequent decay in the crack opening value. In the current research these behaviour is observed. Moreover the capability of simulating high number of fatigue load cycles, makes it possible that this routine is used in the analysis of the effects overloads on the fatigue crack growth.

# 4. FINITE ELEMENT ANALYSIS RESULTS

Contact elements are implemented into the two dimensional elastic plastic finite element analysis of fatigue crack closure. The finite element analyses are carried out using the center crack geometry and the elastic perfectly plastic material properties. The finite element model basics are explained in chapter 3.1. and the model geometry can be seen in figure 3.2. The maximum and minimum loads are applied in cycles and the crack is advanced incrementally at maximum load. For the determination of the crack opening value a routine is developed and it is applied at predetermined load cycle intervals. With the use of these newly developed methods high number of load cycles are simulated.

This chapter starts with presentation of the crack opening stress value results, crack profile changes as the crack advances both at maximum load and at minimum load. Similarly the changes in the plastic zone as the crack is advancing are plotted. The contact element normal force values at minimum load are presented. The same results are shown for plane stress analyses. Than the chapter continues showing the effect of the parameters that are newly introduced are investigated. These are the effect of the number increments of the applied load, the effect of the load cycle interval where the opening stress values are determined are investigated.

## 4.1. Plane Strain Analysis Results

### 4.1.1. Crack Opening Stress

The results of two dimensional plane strain elastic plastic finite element analysis of fatigue crack closure using contact elements can be seen in Figure 4.1. and Figure 4.2. The normalized crack opening values are plotted against load cycle number. These are the results for the first 20 load cycles, where the crack opening value is determined at every cycle and it can be seen that the crack opening values reach a plateau after passing through the initial forward plastic zone.

The results are shown in Figure 4.2. These are the result obtained by extending the analysis to 100 load cycles where the crack opening stress values are determined at every fifth load cycle after the 20th cycle. It can be seen clearly that the crack opening values decreases after the initial plateau observed in the previous figure and it stabilizes at a lower level.

Contact element results are plotted together with the results of Skinner [7] in Figures 4.3 and 4.4. The results of Skinner[7] are for the first 16 cycles. The results are plotted for the first 20 cycles in Figure 4.3. and the results for the first 100 cycles are plooted in figure 4.4. The results are seen to be in good agreement wit each other for the first 16 load cycles. But since Skinner's[7] simulation stops at an early stage the subsequent drop in the stabilization level can not be observed in his work.

Since the newly developed analysis provides the capability of evaluating crack opening stress values at cyclic intervals rather than evaluating crack opening stress values at each cycle, it was possible to observe the crack opening behavior for a prolonged period with appreciably less execution time. While the execution times of both the method of Skinner[7] and the present method with the evaluation of crack opening stress at every load cycle are comparable, the execution time for a 100 cycle analysis with the present method evaluating crack opening stress values at every fifth cycle is approximately one third of the execution time required by the method of Skinner. The execution times for a 10 cycle simulation are listed in Table 4.1. The computer used for the comparison has a CPU of 1.8 GHz, and the RAM is 512 MB.

Table 4.1. Execution time comparison of the present model with the model of Skinner [7] ran on the same computer.

| Method | Time |
|---|---|
| Skinner [7] | 36 min 1 sec |
| Present method (every cycle) | 29 min 17 sec |
| Present method (every 5th cycle) | 12 min 28 sec |

### 4.1.2. Crack Profile and Contact stress

The change in the crack surface profile is monitored. The crack surface profiles at the maximum applied stress are plotted in Figures 4.5, 4.6, and 4.7. for the first, 20th and 100th load cycles, respectively.

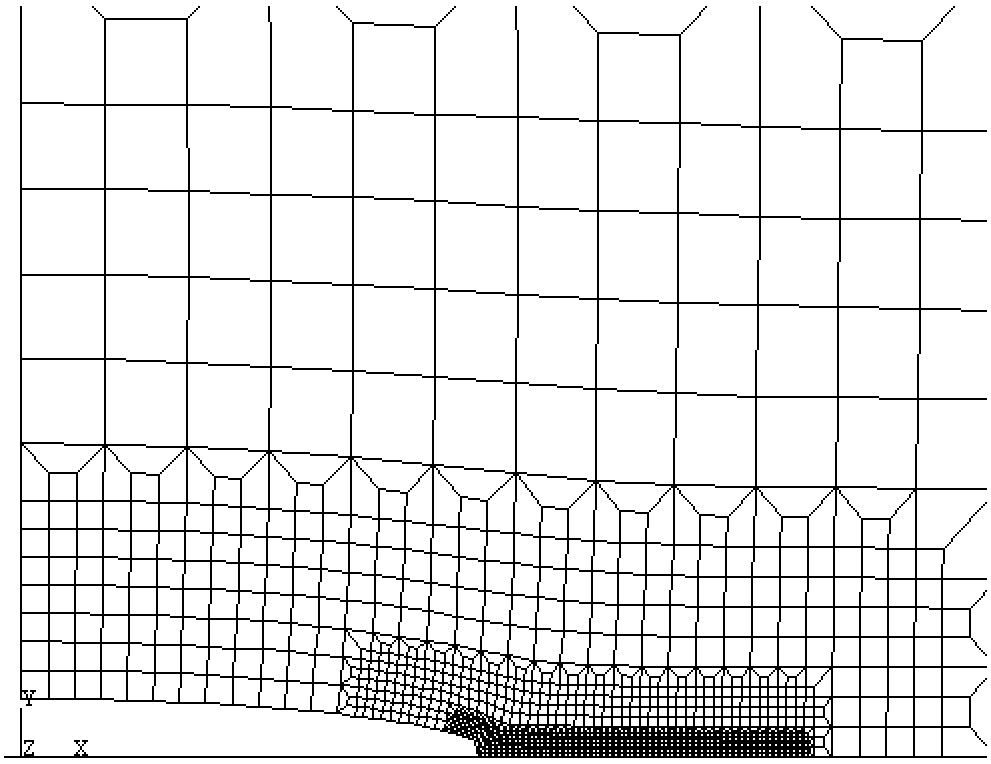


Figure 4.5. Crack surface profile at maximum load at first load cycle.

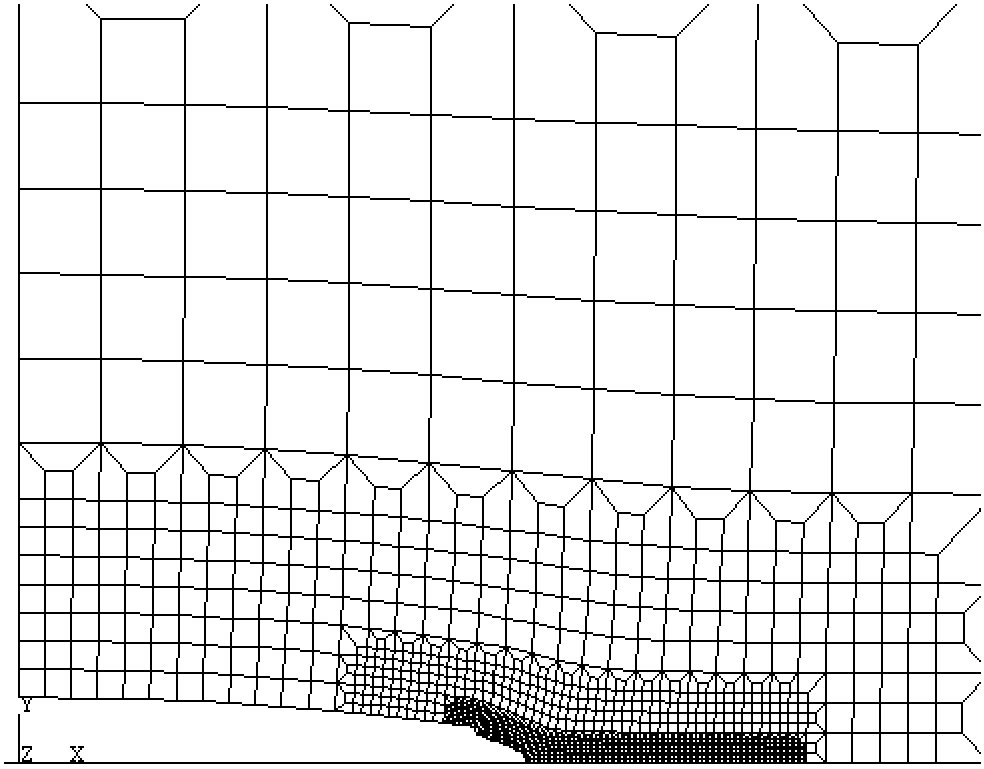


Figure 4.6. Crack surface profile at maximum load at 20th load cycle.

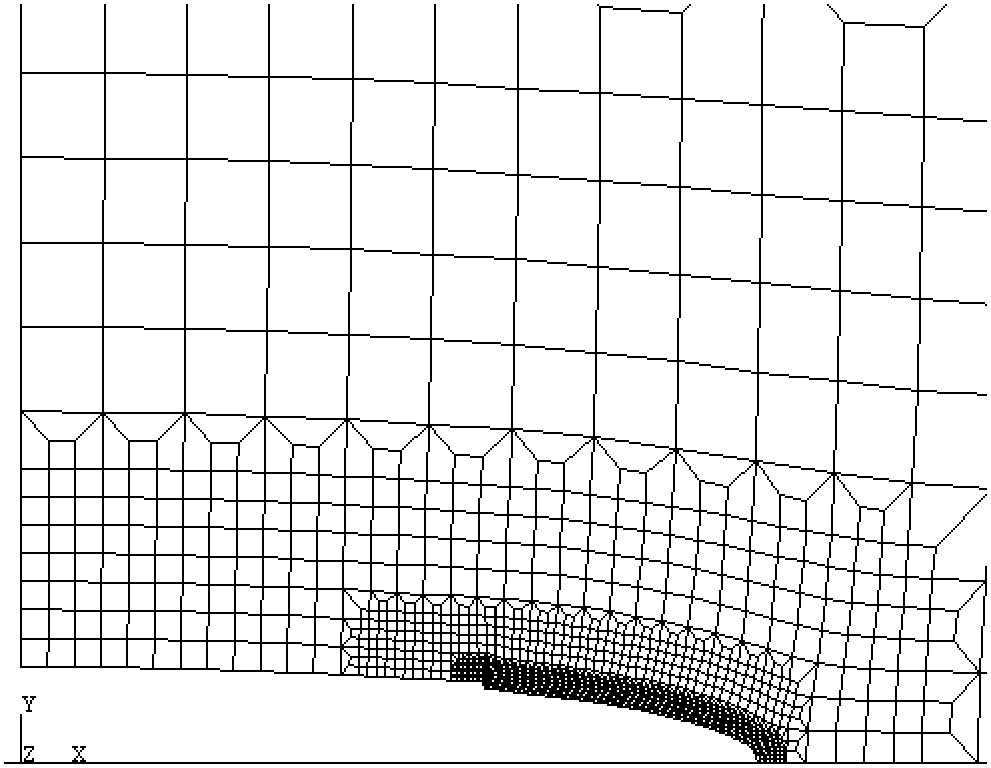


Figure 4.7. Crack surface profile at maximum load at 100th load cycle.

As a summary crack surface profiles at maximum load for the first, 20th and 100th load cycles are plotted together below, in Figure 4.8.

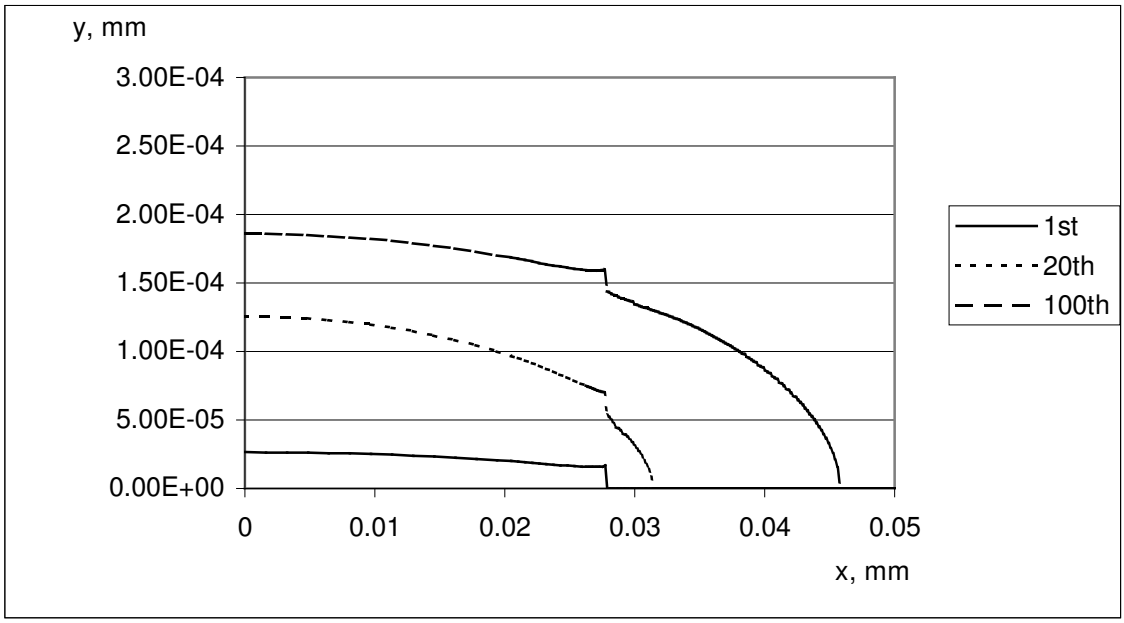


Figure 4.8. Crack surface profiles at maximum load for the first, 20th and 100th load cycles are plotted together.

At the maximum load the plastic zone is identified by plotting the stress contour, where the equivalent von Mises stress value is equal to the yield stress. These plastic zone are plotted together for the first, 20th and the 100th load cycles when the maximum load is applied (Figure 4.9.) . It can be seen how the plastic zone changes as the crack advances. The plastic zones generated at maximum stress increases as the crack increases, which turns out to be as expected.

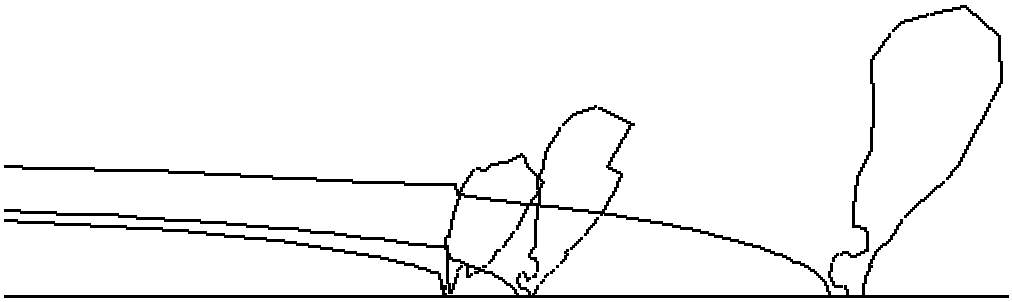

Figure 4.9. Plastic zone change as the crack advances for plane strain geometry.

The crack surface profiles at the minimum applied stress for the first, 20th and 100th load cycles are plotted together in Figure 4.10. It can be seen that the contact occurs mainly at the hump generated when the first load is applied. The first load creates an initial plastic deformation, which is assumed to be responsible for the hump. Therefore the crack closes earlier and the plasticity induced crack closure behavior is observed.

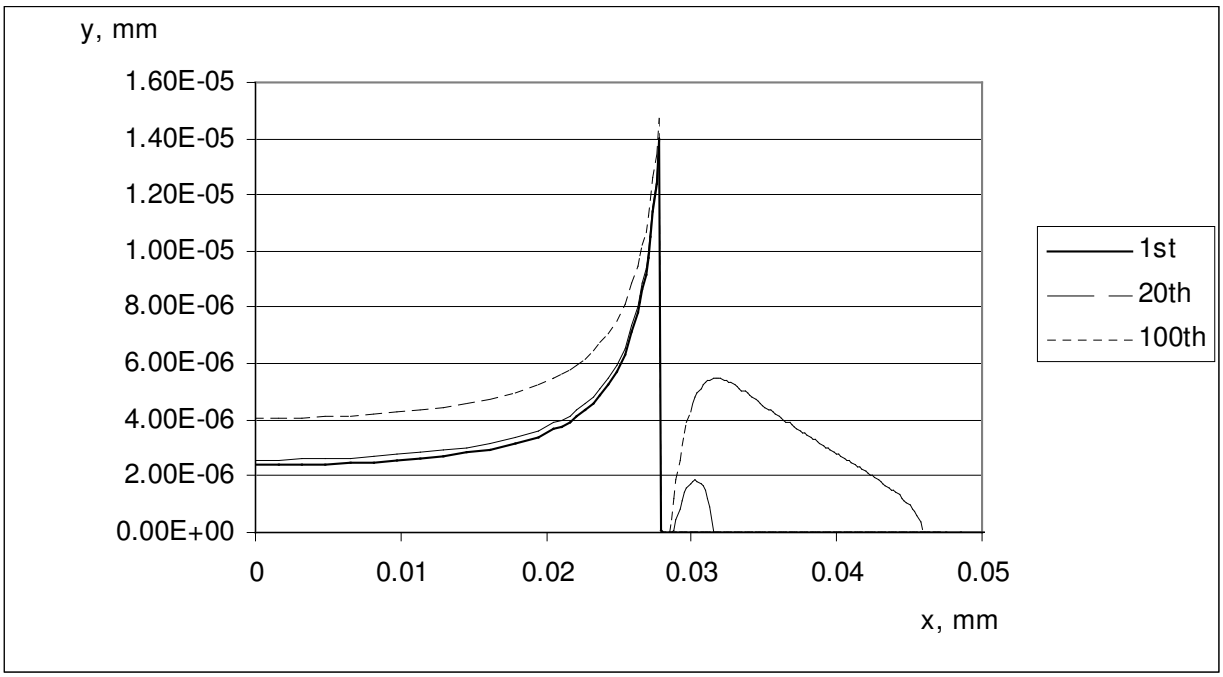


Figure 4.10. Crack surface profiles at minimum load for the first, 20th and 100th load cycles are plotted together.

The normal stress values of the contact elements at minimum loads are shown in Figures 4.11., 4.12 and 4.13, for the first, 20th and 100th load cycles, respectively. The normal stress values can also be called as the contact stress. Note that in these graphs, while the positive part shows the crack surface profile in millimeters, the negative values show the contact stress values.

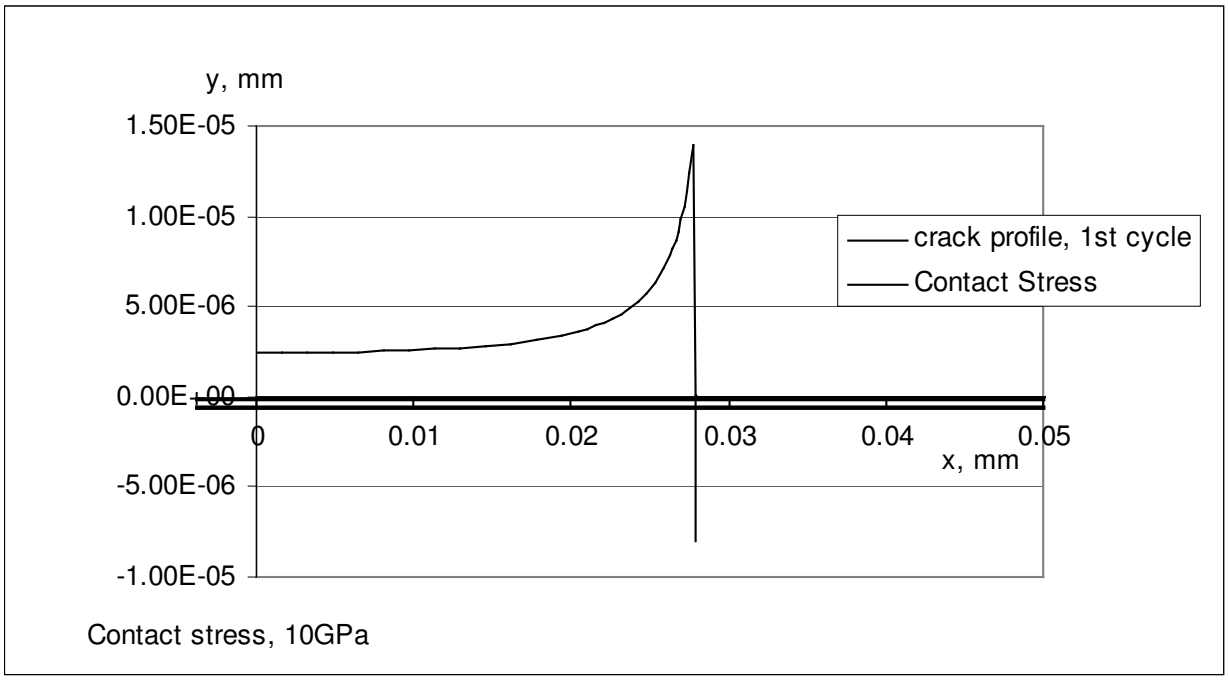


Figure 4.11. The crack surface profile and the contact stress values for minimum load at 1st load cycle. Positive values are for crack surface profile, negative values are contact stress.

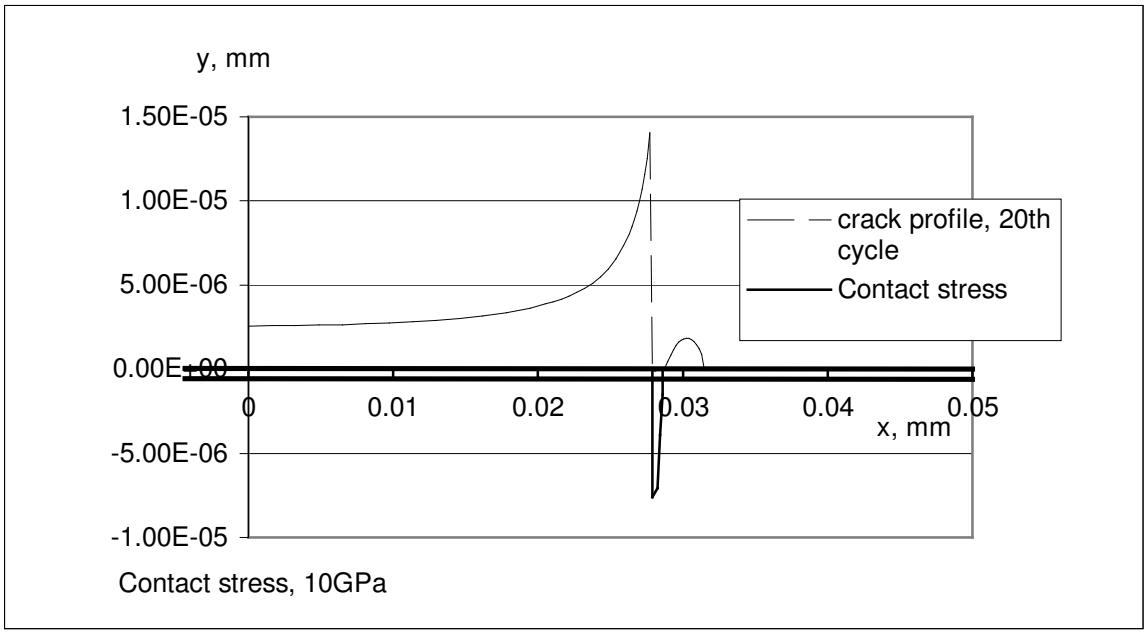


Figure 4.12. The crack surface profile and the contact stress values for minimum load at 20th load cycle. Positive values are for crack surface profile, negative values are contact stress.

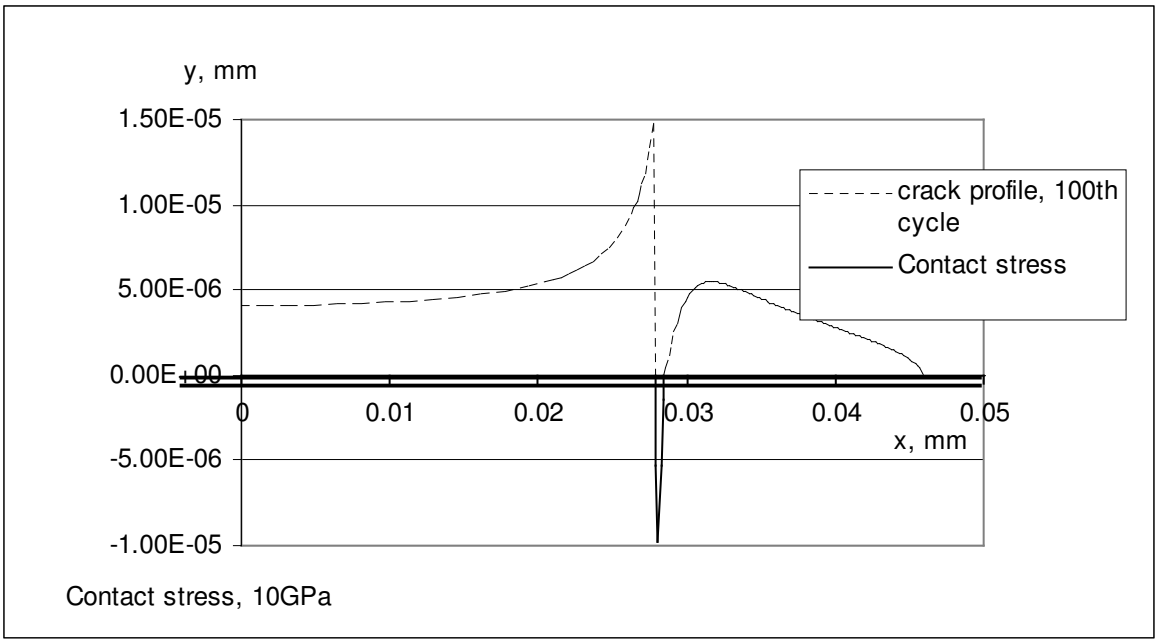


Figure 4.13. The crack surface profile and the contact stress values for minimum load at 100th load cycle. Positive values are for crack surface profile, negative values are contact stress.

## 4.2. Plane Stress Analysis Results

### 4.2.1. Crack Opening Stress

The results of two dimensional plane stress elastic plastic finite element analysis of fatigue crack closure using contact elements can be seen in Figure 4.14. The normalized crack opening values are plotted against load cycle number. These are the results for 25 load cycles, where the crack opening value is determined at every cycle and it can be seen that the crack opening values reach a plateau after passing through the initial forward plastic zone. As stated in the literature the plane stress crack opening stress values should be higher than the values for plane strain. Plane strain and plane stress analysis results are compared in Figure 4.15.

### 4.2.2. Crack Profile and Contact Stress

The change in the crack surface profile is monitored. The crack surface profiles at the maximum applied stress are plotted in Figures 4.16, 4.17, and 4.18. for the first, 15th and 25th load cycles, respectively.

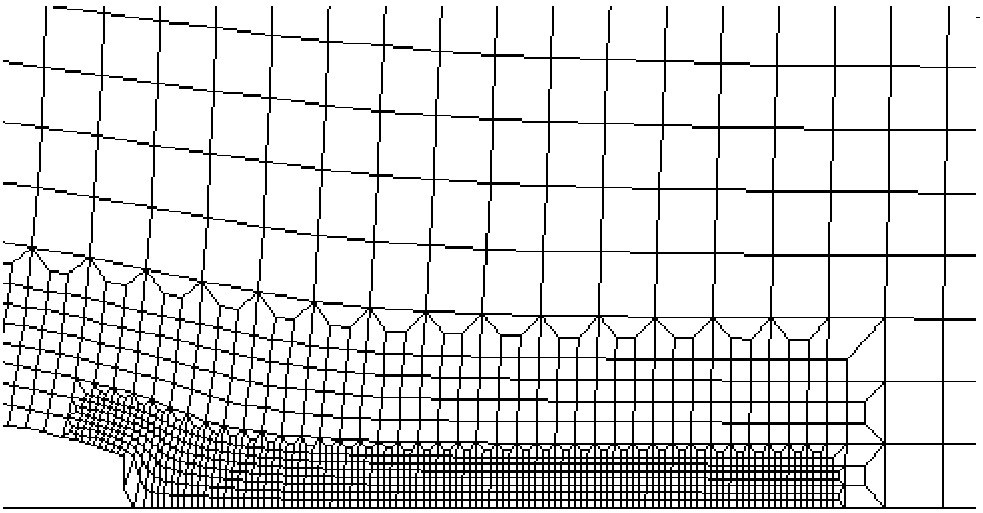

Figure 4.16. Crack surface profile at minimum load at 1st load cycle for plane stress analysis.

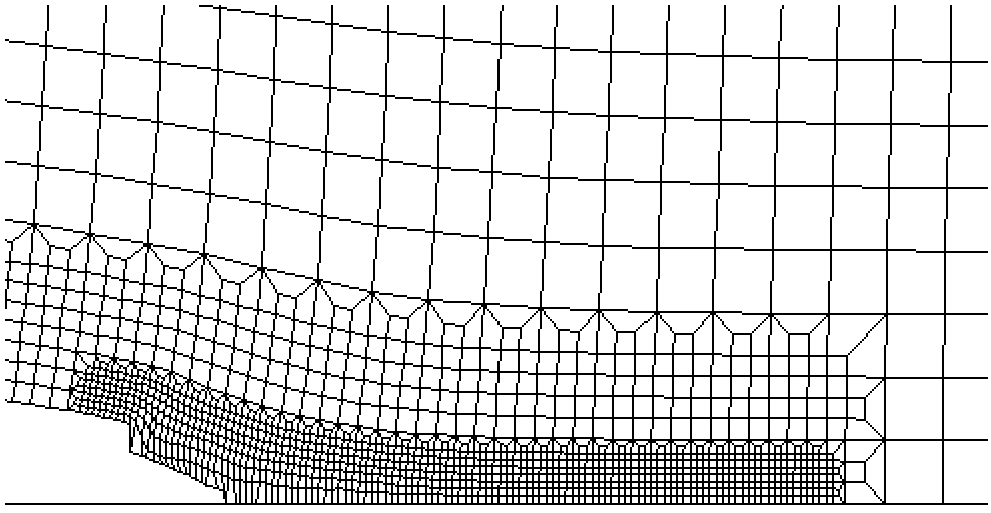

Figure 4.17. Crack surface profile at minimum load at 15th load cycle for plane stress analysis.

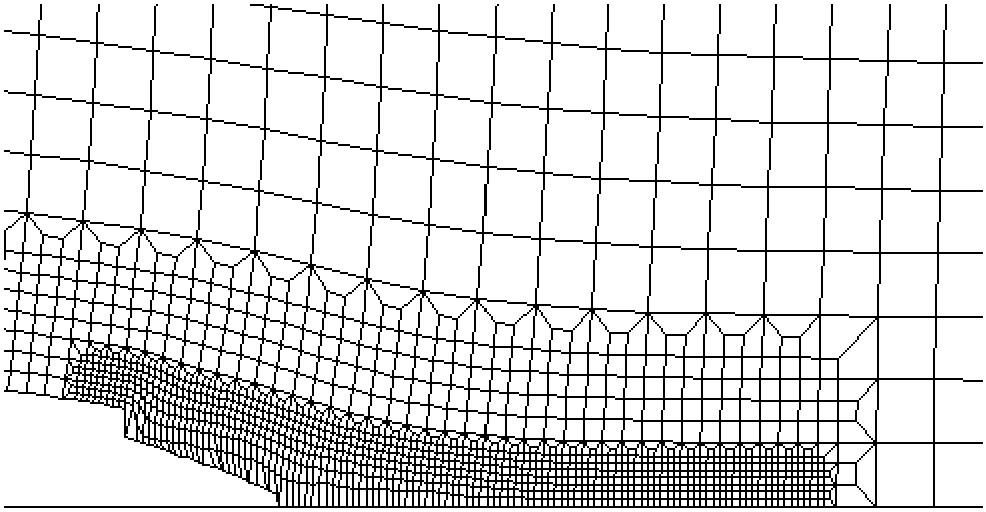

Figure 4.18. Crack surface profile at minimum load at 25th load cycle for plane stress analysis.

As a summary crack surface profiles at maximum load for the first, 20th and 100th load cycles are plotted together below, in Figure 4.19.

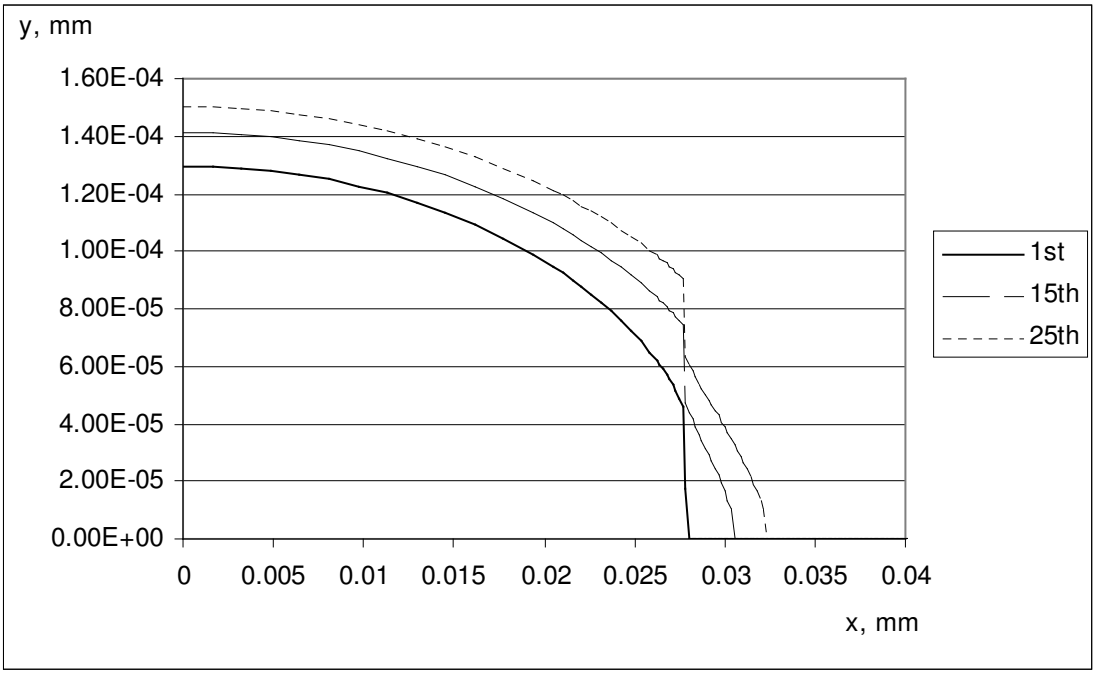


Figure 4.19. Crack surface profiles at minimum load for the first, 15th and 25th load cycles are plotted together for plane stress analysis.

The crack surface profiles at the minimum applied stress for the first, 15th and 25th load cycles are plotted together in Figure 4.20. It can be seen that the contact occurs mainly near the crack tip. A hump is not developed as it was developed in plane strain conditions.

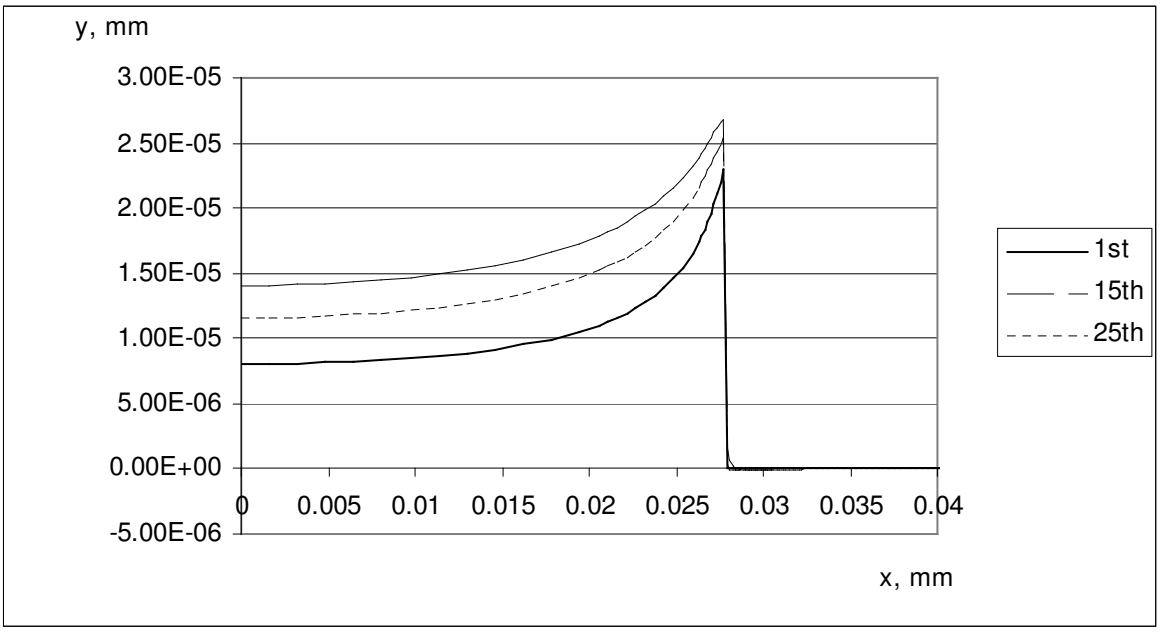


Figure 4.20. Crack surface profiles at minimum load for the first, 15th and 25th load cycles are plotted together.

The normal stress values of the contact elements at minimum loads are shown in Figures 4.21., 4.22 and 4.23, for the first, 15th and 25th load cycles, respectively. Note that in these graphs, while the positive part shows the crack surface profile in millimeters, the negative values show the contact stress values.

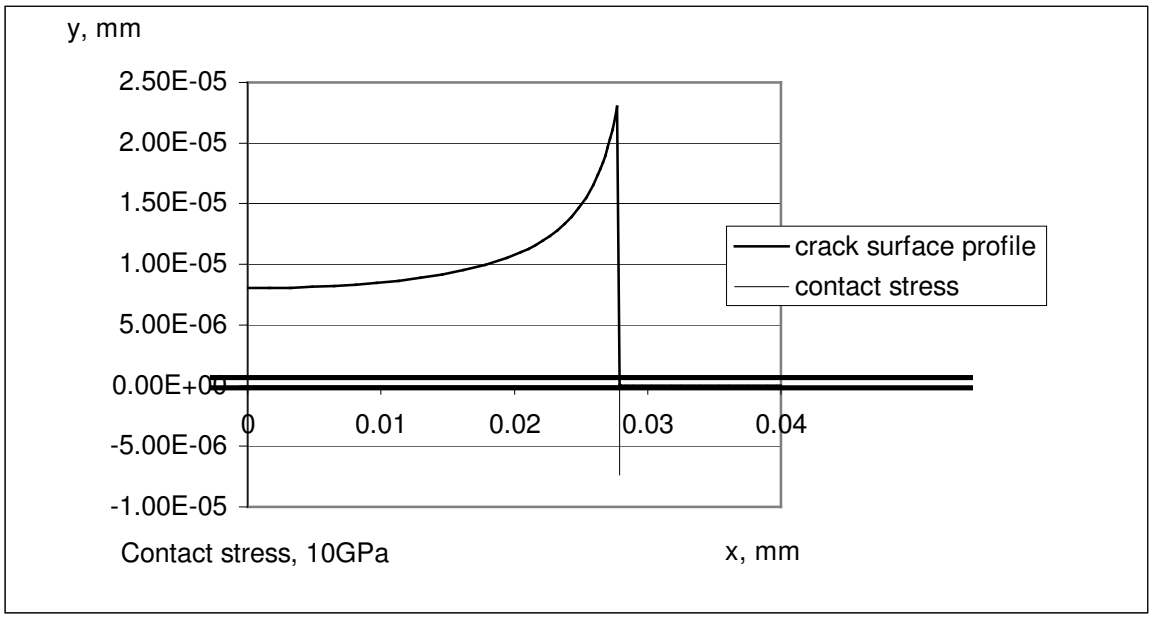


Figure 4.21. The crack surface profile and the contact stress values for minimum load at 1st load cycle for plane stress analyses. Positive values are for crack surface profile, negative values are contact stress.

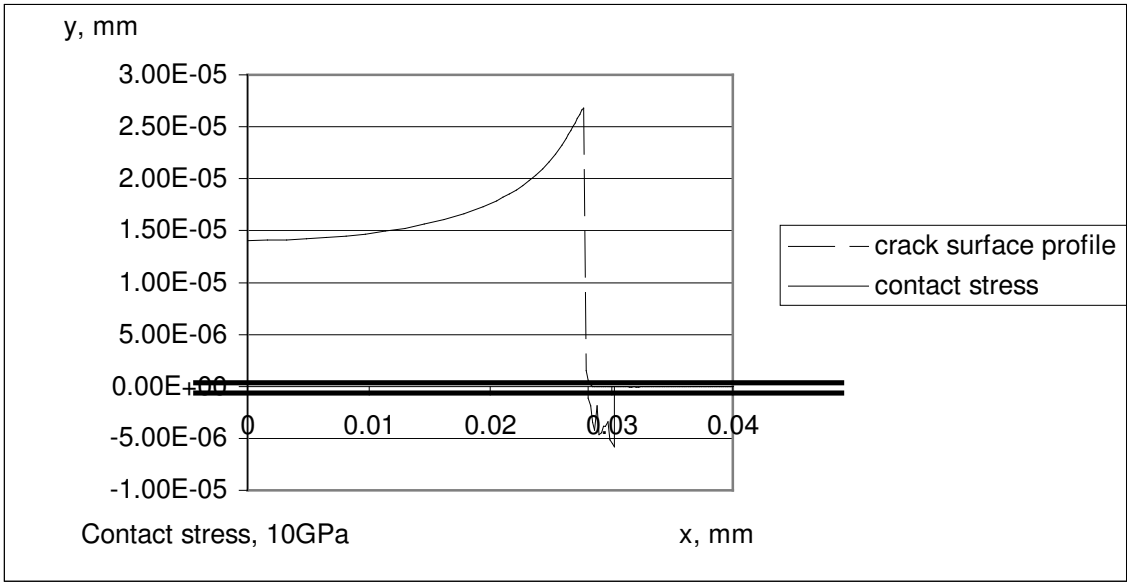


Figure 4.22. The crack surface profile and the contact stress values for minimum load at 15th load cycle for plane stress analyses. Positive values are for crack surface profile, negative values are contact stress.

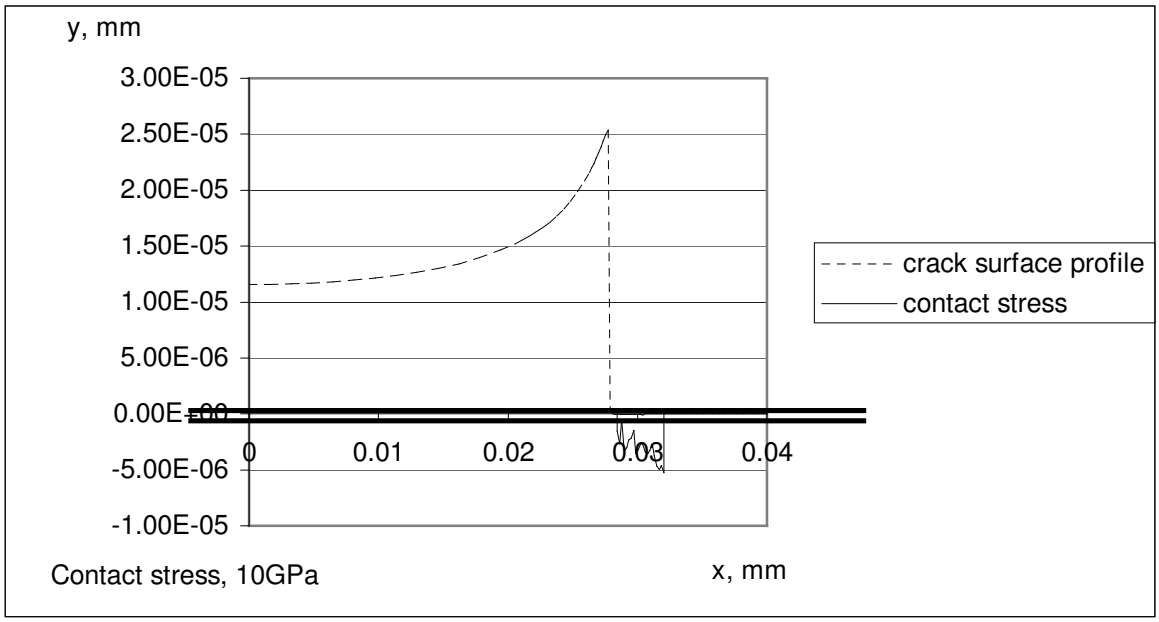


Figure 4.23. The crack surface profile and the contact stress values for minimum load at 25th load cycle for plane stress analyses. Positive values are for crack surface profile, negative values are contact stress.

### 4.3. Effect of Related Parameters

The new parameters related to the implementation of contact elements and to the developed routine for the determination of closure opening stress values are investigated. Te results presented here are for the plane strain elastic-plastic finite element analysis of center cracked specimen.

According to the newly developed algorithm, the crack opening stress value can be determined at predetermined load cycle intervals. The effect of the load cycle intervals is shown in figure 4.24. Since all the data points coincide, and the values are exactly the same, the load cycle interval does not have an effect on the results.

The determination crack opening level can be accomplished by applying the load in increments, which may be called as the resolution of the opening stress evaluation. The effect of the resolution while determining crack opening stress is shown in Figures 4.25. and 4.26. The analysis shows that the resolution has negligible effect on the results.

# 5. CONCLUSION

Contact elements are implemented into the finite element analysis of fatigue crack closure to predict crack opening stress values, by developing a code using ANSYS Parametric Design Language(APDL).

A routine is developed to determine crack opening stress values at predetermined load cycles. Since the newly developed analysis provides the capability of evaluating crack opening stress values at cyclic intervals rather than evaluating crack opening stress values at each cycle, it was possible to observe the crack opening behavior for a prolonged period with appreciably less execution time. While the execution times of both the method of Skinner[7] and the present method with the evaluation of crack opening stress at every load cycle are comparable, the execution time with the present method with crack opening stress values evaluated at every fifth cycle is approximately one third of the execution time required by the method of Skinner.

With the possibility of observing crack closure behavior for a large number of load cycles, typically 100, it was observed that following an initial stabilization after the crack has progressed through initial forward plastic zone, a subsequent decay and further stabilization is occurred.

Plane stress analyses are carried out and are compared with the plane strain analysis results. It can be seen that, as expected, the plane stress crack opening values are higher and stabilize earlier.

Plasticity induced fatigue crack closure occurs because of the plastic deformation near the crack tip. Therefore the crack surface profiles both at maximum load and minimum load are plotted as the crack is advanced. The hump generated by the initial load is the main cause of crack closure in plane strain, whereas in plane stress analyses the closure occurs behind the crack close to the crack tip. Contact stress values support this observation.

The newly introduced parameters related to the implementation of contact elements are investigated. The effect of the load application increments, which can be thought as a resolution, has negligible effect on the determination crack opening stress. The load cycle interval, at which crack opening stress is evaluated, has no effect on the results.

As a further research the model can be extended to model three dimensional fatigue crack closure. With the capability of simulating high number of load cycles, the present model can be used as a tool for the investigation of the effects of overloads in fatigue crack growth.

# APPENDIX

The code written in ANSYS Parametric Design Language (APDL) for the modeling of fatigue crack closure with contact elements is presented here. The code consists of several modules. Each module is listed in the following pages.

Main code
appbcs.mac
strtcyc.mac
firstload.mac
appload.mac
selctnodes.mac
advancecrack.mac
clearrst.mac
lload.mac
unnload.mac
loadcrack.mac
recover.mac

## Main Code

```
!/batch
/FILNAM,cl05
/title, crack closure05
/output,sopresult,txt,,append
  *vwrite,'2d_psn_','100_pcg'
(a8,a8)

/output !---------------------------------------loading
strsMax=150e6
strsMin=0

!---------------------------------------number of load cycles
nlc=3

!---------------------------------------- geometry

! t thickness; w width;
! c crack length x
! a crack length z
! da crack advance

t=0
w= 0.230
height= 0.460
c=0.0279
!c=0.023
a=0
da=0.00018
```

```
!----------------------------------------material properites
E=70e9
YS=350e6
HTAN=0

! ----------------------------------------mtype
! 2D :center cracked 2-D
! TC :center cracked 3-D

mtype='2D'


! crack growth parameters
! ncgecut   number of cuts to nodal reaction force during crack advance
! cgerf factor to reduce nodal reaction force during advance nodeforce= nodeforce/cgerf

ncgecut=5
cgerf=2

!-----------------------------------------------------------jobname

*get,JN,active,,jobnam

!-----------------------------------------------------apply boundary conditions

AppBcs


! ------------------------------------------------file system

! bdrive: drive
! bdir : dir for back-up after every load step
```

```
! maxdir :back-up at max load
! mindir :backup at min load

bdrive='c:'
bdir='\backup'
maxdir='\maxload'
mindir='\minload'
advdir='\adv'
Sopdir='\Sop'
sopmdir='\Sopm'
workdir='\ansyswd'
rundir1='\run'
rundir2='\0808'


/solu

! load increments as percentage of range (smax-smin)

! libco :loading, before any node opening
! lidco :loading, during crack opening
! liaco :loading, crack is fully open
! uibcc :unloading, before any node closes
! uidcc :unloading, during crack closing
! uiacc :unloading, crack is fully closed

libco=0.05
lidco=0.025
liaco=0.10
uibcc=0.05
uidcc=0.025
uiacc=0.10
```

```
!-----------------------------------------non linear options----------------
solcontrol,on
nsub,1
neqit,500
nropt,full,,on
eqslv,pcg,1.0e-4

!resume control ansys 5.6 or greater

!rescontrl,define,none,none

!-------------------------------------------------------start

nlc=100

StrtCyc
```

**appbcs.mac**

```
/prep7

shpp,off

!--------------bilinear kinematic hardening
mp,ex,1,E
tb,bkin,1,1,1,,
tbmodif,2,1,ys
tbmodif,3,1,htan

!-------------------------------------------------look
*if,mtype,eq,'2D',then
 et,1,plane42,,,2,,
 !  kopt(3)=0    ! plane stress
 !  kopt(3)=2    ! plane strain
 !  kopt(3)=3   ! plane stress w thickness
*else
 et,1,solid45,,,,,
*endif

! read node and elem data
mat,1,
type,1
real,1

!-----------------------------------------
NRRANG,1,999999,1,
NREAD,meshh,cdr,,

ERRANG,1,999999,1,
```

```
eread,meshh,elm

nsel,s,loc,y,0
nsel,r,loc,x,c,1000000
nsel,u,loc,x,0,c-da*0.25
d,all,uy,0

! block for negative R
nsel,s,loc,y,0
nsel,r,loc,x,0,c
nsel,u,loc,x,c-0.3*da,c+0.3*da
cm,csnodes,node
! x direction

nsel,s,loc,x,0
d,all,ux,0
nsel,all



! 3d z direction

! nsel,s,loc,z,0
!d,all,uz,0
!nsel,all

! crack mouth nodes ..cmnodes
nsel,s,loc,x,0
nsel,r,loc,y,0
cm,cmnodes,nodes

cmsel,all
nsel,all
esel,all
```

```
! create contact elements--------------------

ET,2,CONTAC26,0
R,2,1e12, , ,
!R,1,1e10,,0,1e8
type,2
real,2
wdt=0.2
*get,ground1,node,,num,max
ground1=ground1+1
ground2=ground1+1
n,ground1,-0.001,0
n,ground2,wdt,0
nsel,s,loc,y,0
nsel,r,loc,x,0,wdt

*get,nsnodes,node,,count

nodno=0
*do,jj,1,nsnodes
  nodno=ndnext(nodno)
  *if,nodno,ne,ground1,then
     *if,nodno,ne,ground2,then
    e,nodno,ground1,ground2
     *endif
  *endif
*enddo

!/prep7
! modify real constants
!nsel,s,loc,y,0
```

```
!nsel,r,loc,x,c,1000000
!nsel,u,loc,x,0,c-da*0.25
!nsel,u,,,ground2
!ESLN,S
!ESEL,R,TYPE,,2
!EMODIF,all,REAL,2,

nsel,all

d,ground1,ALL ,0,
d,ground2,ALL ,0,

!_______end of contact elements

cmsel,all
esel,all
nsel,all
!wsort,all,0

save
```

**strtcyc.mac**

```
!nlc total number of load cycles
!nls number of intervals for s zero


autots,off
!number of substeps
stepno=5

/output,status,txt,,
*vwrite,'1. load','start'
(a10,a10)
/output

firstload


clearrst,bdrive,bdir,maxdir

/output,status,txt,,append
*vwrite,'1. load','end'
(a10a10)
/output

/post1
/SHOW,file,grph,
/GFILE,600,
/DEVICE,VECTOR,1
/PLOPTS,MINM,0
/PLOPTS,INFO,1
/PLOPTS,LEG1,1
```

```
/PLOPTS,LEG2,1
/PLOPTS,LEG3,1
/PLOPTS,FRAME,1
/PLOPTS,TITLE,1
/PLOPTS,MINM,0
/PLOPTS,LOGO,0
/PLOPTS,WINS,1
/PLOPTS,WP,0
/TRIAD,ORIG
eplot
/CLABEL,1,-1
/DSCALE,1,30
/CVAL,1,349e6,
/CLABEL,1,-1
/focus,1,0.036,0
/DIST, 1 ,1/18,1
replot
!
PLDISP,0
PLNSOL,S,EQV,0,1
finish
/SHOW,term
/solu

ij=0

*do,i,1,nlc

*if ,i,le,20,then
nls=1
*endif
*if ,i,gt,20,then
nls=5
```

```
*endif

  ij=ij+1
          /output,status,txt,,append
  *vwrite,'advance',i,'start'
(a10, f5.0,a10)
  /output

  advancecrack,i

  /output,status,txt,,append
  *vwrite,'advance',i,'end'
(a10, f5.0,a10)
  /output

  clearrst,bdrive,bdir,advdir

/output,status,txt,,append
  *vwrite,'unload',i,'start'
(a10, f5.0,a10)
  /output

  unnload,i

  /output,status,txt,,append
  *vwrite,'unload',i,'end'
(a10, f5.0,a10)
  /output

  clearrst,bdrive,bdir,mindir

  *if ,ij,eq,nls,then
```

```
  /output,status,txt,,append
  *vwrite,'-load-So',i,'start'
(a10, f5.0,a10)
  /output

save, Smin%i%%jn%,db
/prep7
wsort,all,0
/solu


      loadcrack,i


  /output,status,txt,,append
  *vwrite,'-load-So',i,'end'
(a10, f5.0,a10)
  /output

!     recover emat (0 th state) "one shot loading"
finish
/del,JN,emat,
/del,JN,esav,
/del,JN,db

/copy,minn,emat,,JN,,
/copy,minn,esav,,JN,,
/copy,minn,db,,JN,,
/del,minn,emat,
/del,minn,esav,
/del,minn,db
```

```
/solu
resume
parres,,minn,par

      ij=0
  *endif

  /output,status,txt,,append
  *vwrite,'load',i,'start'
(a10, f5.0,a10)
/output

/prep7
wsort,all,0
/solu
      lload,i

*if ,ij,eq,0,then
save, Smax%i%%jn%,db

/post1
PLNSOL,S,EQV,0,1
/SHOW,file,grph,
/DEVICE,VECTOR,1
replot
/SHOW,term
finish

*endif
  /output,status,txt,,append
  *vwrite,'load',i,'end'
(a10, f5.0,a10)
```

```
  /output

  clearrst,bdrive,bdir,maxdir

*enddo
```

**firstload.mac**

```
! apply max load on first cycle

! calculate elastic limit

!/solu
!appload,height,1
!autots,off
!solve
!/post1
!nsort,s,eqv,1,0
!*get,maxstrs,sort,max
!/solu
!appload,height,ys/maxstrs
!time,(ys/maxstrs)*0.45,/(strsmax)
!solve
!save

appload,height,strsmax
!autots,on
nsubst,stepno
time,0.45
nsel,all
esel,all
solve
save
```

**appload.mac**

```
! usage
! appload,height, pressure

nsel,s,loc,y,arg1
!d,all,uy,arg2
sf,all,pres,(-1)*arg2
nsel,all
```

**selctnodes.mac**

```
! to select nodes at the crack tip at load cycle N
! usage
!  selctnodes,n

nsel,s,loc,y,0
nsel,r,loc,x,c+da*(arg1-1.25),c+(arg1-0.75)*da



! local,11,1,0,0,0,0,90,0,(a+da*(arg1-1))/(c+da*(arg1-1))
! nsel,s,loc,x,c+da*(arg1-1.45)*da,c+(arg1-0.55)*da
! nsel,r,loc,z,0
!csys,0
```

**advancecrack.mac**

```
! advane crack uniformly by one element

! syntax Advancecrack, loadcyclenumber
/solu

nsubst,1,1,1

selctnodes,arg1
*get,nnodes,node,,count
nodno=0

*do,jj,1,nnodes
      nodno=ndnext(nodno)
      *get,noderf,node,nodno,rf,fy
      ddele,nodno,uy
!       f,nodno,fy,noderf
*enddo
nsel,all
esel,all

!R,2,10,
!timevar=0.45+0.05/(ncgecut+1)+(arg1-1)
!time,timevar
!solve
!save

*do,j,1,ncgecut-1

  selctnodes,arg1
  nodno=0
```

```
  *do,jj,1,nnodes
     nodno=ndnext(nodno)
     *get,noderf,node,nodno,f,fy
     f,nodno,fy,noderf/cgerf
  *enddo
  nsel,all
  esel,all
finish

  /solu
 antype,,rest
 timevar=0.45+(j+1)*0.05/(ncgecut+1)+(arg1-1)
 time,timevar
 solve
 save
*enddo



selctnodes,arg1
nodno=0
*do,jj,1,nnodes
   nodno=ndnext(nodno)
   *get,noderf,node,nodno,f,fy
   fdele,nodno,fy
*enddo
nsel,all
esel,all
finish

 /solu
antype,,rest
timevar=(arg1-0.5)
```

```
time,timevar
solve
save


! modify real constant

!/prep7
!selctnodes,arg1

!ESLN,S
!ESEL,R,TYPE,,2
!EMODIF,all,REAL,1,
!/solu
!esel,all
!nsel,all
```

**clearrst.mac**

```
! to save disk space
! deletes *.rst
! usage
! clearrst,bdrive,bdir1,bdir2
! clearrst,bdrive,bdir1,"

finish
!pltzone
!/copy,,rst,,,,%arg1%%arg2%%arg3%

/copy,,emat,,,,%arg1%%arg2%%arg3%
!/copy,,osav,,,,%arg1%%arg2%%arg3%
/copy,,esav,,,,%arg1%%arg2%%arg3%
!/copy,,mntr,,,,%arg1%%arg2%%arg3%
/copy,,db,,,,%arg1%%arg2%%arg3%
/delete,,rst
/solu
antype,,rest
```

**lload.mac**

```
! apply max load

/solu
appload,height,strsmax
!autots,on
nsubst,stepno
nsel,all
esel,all
time,arg1+0.45
solve
save
```

**unnload.mac**

```
! apply min load

!R,1,1e10, ,0,1e7,
appload,height,strsmin
!autots,on
nsubst,stepno
nsel,all
esel,all
time,arg1

solve
save
```

**loadcrack.mac**

```
! loadcrack


! determination crack opening stress

!            smaxlim
!          /  5
!        /  4
!      /  3
!    /  2
!  /  1
! sminlim
!
! slevel: refinement  (1) 5x  (2) 5x  (3) 4x
! stepcnt: step at each slevel
! divider  max step at each slevel
! ijk  do loop counter, actually dummy
! openstat: state of contact elements: 0 closed, 1 open
! cumforce: cumulative force to detect whether all elements are open
! a folder is needed..:Sop

smaxlim=strsmax
sminlim=strsmin

stepcnt=0
slevel=0
divider=5
openstat=0
cumforce=0
```

```
!record for backup, ----------------------------------------------------------------
finish
! /copy, fname1,ext1,dir1, fname2, ext2, dir2

save
parsav,,minn,par

/copy,JN,emat,,min,,
/copy,JN,esav,,min,,
/copy,JN,db,,min,,
/copy,JN,emat,,minn,,
/copy,JN,esav,,minn,,
/copy,JN,db,,minn,,

finish
/solu

nsubst,2,2,2

/output,status,txt,,append
*vwrite,'S opening'
(a10)
*vwrite,'-----------'
(a10)
/output

*do,ijk,1,15

!       recover emat file ---------------------------------- ---------------------------------
finish

parsav,,min,par
/del,JN,emat,
```

```
/del,JN,esav,
/del,JN,db
/copy,min,emat,,JN,,
/copy,min,esav,,JN,,
/copy,min,db,,JN,,
/solu

resume,,,,
parres,,min,par

   stepcnt=stepcnt+1
   sdelta=(smaxlim-sminlim)/divider
   s=sdelta*stepcnt+sminlim

/solu
   appload,height,s
    nsel,all
    esel,all
finish
/solu
antype,,rest
    solve
!    save, Sop%ijk%,db  ------------------------------------------------------------
    save

finish
/del,cur,emat,
/del,cur,esav,
/del,cur,db
    /copy,JN,emat,,cur,,
    /copy,JN,esav,,cur,,
    /copy,JN,db,,cur,,
```

```
/solu
!
!--------------------   check contact elements        openstat=0 or 1 (explicitly)

 esel,all

/post1
  ESEL,S,TYPE,,2
  *get,nselem,elem,,count
  elemno=0

  /output,status,txt,,append
*vwrite,'--------',
(a10)
*vwrite,'smaxlim:',smaxlim
(a10, f30.1)
*vwrite,'sminlim:',sminlim
(a10, f30.1)
*vwrite,'sdelta:',sdelta
(a10, f30.1)
*vwrite,'divider:',divider
(a10, f30.1)
*vwrite,'stepcount:',stepcnt
(a10, f30.1)
*vwrite,'steplvl:',slevel
(a10, f30.1)
*vwrite,'s:',s
(a10, f30.1)

  /output

cumforce=0
            *do,jjj,1,nselem
```

```
                elemno=elnext(elemno)

!               *get,elemgap,elem,elemno,nmisc,3
                *get,elemf,elem,elemno,smisc,1

!               *get,nodno,elem,elemno,node,1
!               nxloc=nx(nodno)
!               ndang=nz(nodno)
!               nodestat=0
                cumforce=cumforce+elemf
              *enddo

   *if,cumforce,lt,0,then
  openstat=0
   *else
  openstat=1
    *endif

  /output,status,txt,,append
*vwrite,'cumforc:',cumforce
(a10, f30.1)
*vwrite,'openstat:',openstat
(a10, f30.1)
  /output


!--------------------   check contact elements        openstat=0 or 1 (explicitly)

   *if,openstat,eq,0,then
finish
```

```
/del,JN,rst
/del,min,emat,
/del,min,esav,
/del,min,db
/copy,cur,emat,,min,,
/copy,cur,esav,,min,,
/copy,cur,db,,min,,
/post1
   *endif


   *if,openstat,eq,1,then
      sminlim=s-sdelta
      smaxlim=s
!     recover emat file

      cumforce=0

finish
/solu
antype,,rest

! ..............................

      stepcnt=0
      slevel=slevel+1
    *endif

    *if,slevel,eq,2, then
       divider=4
     *endif
```

```
     *if,slevel,eq,3,then
!       write   s(this step):smaxlim, sprevious step:sminlim
/output,status,txt,,append
  *vwrite,'s(step)','smaxlim','   s prev','smin'
(a10, a10)
  *vwrite,'------',' ','   -------','    '
(a10, a10)

  *vwrite,smaxlim,sminlim
(f30.20, f30.20)

/output

out1=arg1
out2=(smaxlim+sminlim)/2
/output,sopresult,txt,,append

  *vwrite,out1,'.',out2
(f5.0,a1,f30.5)

/output

        *exit
     *endif

! record for backup, delete rst
!clearrst,bdrive,bdir,sopdir

*enddo

finish
/del,cur,emat,
/del,cur,esav,
```

/del,cur,db

/del,min,emat,

/del,min,esav,

/del,min,db

finish

/solu

**recover.mac**

save
finish
!pltzone
!/copy,,rst,,,,%arg1%%arg2%%arg3%

!/copy,,emat,'c:\backup\max3\',,,'c:\ansysworkspace\run\0411closure19\',
!/copy,,osav,'c:\backup\max3\',,,'c:\ansysworkspace\run\0411closure19\',
!/copy,,esav,'c:\backup\max3\',,,'c:\ansysworkspace\run\0411closure19\',
!/copy,,mntr,'c:\backup\max3\',,,'c:\ansysworkspace\run\0411closure19\',
!/copy,,db,'c:\backup\max3\',,,'c:\ansysworkspace\run\0411closure19\',
!/copy,,rst,'c:\backup\max3\',,,'c:\ansysworkspace\run\0411closure19\',
!/copy,,tri,'c:\backup\max3\',,,'c:\ansysworkspace\run\0411closure19\',
!/copy,,full,'c:\backup\max3\',,,'c:\ansysworkspace\run\0411closure19\',

/del,,emat,
/del,,osav,
/del,,esav,
/del,,db
/del,,dbb
/del,,rst
/del,,tri
!/del,,full
!/del,,MNTR

/copy,,emat,%arg1%%arg2%%arg3%,,,%arg4%%arg5%%arg6%%arg7%
/copy,,esav,%arg1%%arg2%%arg3%,,,%arg4%%arg5%%arg6%%arg7%
/copy,,db,%arg1%%arg2%%arg3%,,,%arg4%%arg5%%arg6%%arg7%
parsav

resume,,,,

parres

/solu

antype,,rest

# REFERENCES

1. Stephens, R. I, and Fuchs, H. O., “Metal Fatigue in Engineering”, John Wiley, New York, 1980.

2. Boresi, A. P., Schmidt, R. J., and Sidebottom, O. M., “Advanced Mechanics of Materials”, 5 th Edition, John Wiley., New York,1993.

3. Elber, W., “Fatigue Crack Closure under Cyclic Tension”, Engineering Fracture Mechanics, Vol. 2, pp. 37-45, 1970.

4. Paris, P. C., and Erdogan, F., “A Critical Analysis of Crack Propagation Laws”, Journal of Basic Engineering, pp. 528-534,1963.

5. Gall K., Sehitoglu H., and Kadioglu Y., “Plastic Zones and Fatigue-crack Closure under Plane-strain Double Slip”, Metallurgical and Material Transactions A, Vol. 27(11), pp. 3491-3502, 1996.

6. Anderson, T. L., Fracture Mechanics: Fundamentals and Applications, CRC Press, Boca Raton, 1991.

7. Skinner, J. D., and Daniewicz, S. R., “Simulation of Plasticity-Induced Fatigue Crack Closure in Part-Through Cracked Geometries Using Finite Element Analysis”, Engineering Fracture Mechanics, Vol. 69, pp. 1-11, 2002.

8. McClung, R. C., Thacker, B. H., and Roy S., “Finite Element Visualization of Fatigue Crack Closure in Plane-stress and Plane-strain”, International Journal of Fracture, Vol. 50, pp. 27-49, 1991.

9. Fleck, N. A., “Finite Element Analysis of Plasticity-induced Crack Closure under Plane-strain Conditions”,. Engineering Fracture Mechanics, Vol. 25(4), pp. 441- 449, 1986.

10. Fleck, N. A., and Newman, J. C., “Analysis of Crack Closure under Plane-strain Conditions”, Mechanics of Fatigue Crack Closure ASTM STP 982, pp. 319-341, 1988.

11. Blom, A. F., and Holm, D. K., “An Experimental and Numerical Study of Crack Closure”, Engineering Fracture Mechanics, Vol. 22, pp. 997-1101,1985.

12. Ashbaugh, N. E., Dattaguru, B., Khobaib, M., Nicholas, T., Prakash, R.V., Ramamurthy, T. S., Seshadri, B. R., and Sunder R., “Experimental and Analytical Estimates of Fatigue Crack Closure in an Aluminum-copper Alloy Part II: A Finite Element Analysis”, Fatigue and Facture in Engineering Materials and Structure, Vol. 20(7), pp. 963-974, 1997.

13. Dougherty, J. D., Padovan, J., and Srivatsan, T. S., “Fatigue Crack Propagation and Closure Behavior of Modified 1071 Steel: Finite Element Study”, Engineering Fracture Mechanics, Vol. 56(2), pp. 189-212, 1997.

14. Pommier, S., “Plane Strain Crack Closure and Cyclic Hardening”, Engineering Fracture Mechanics, Vol. 69, pp. 25-44, 2001.

15. Sehitoglu, H., and Sun, W., “Modeling of Plane Strain Fatigue Crack Closure”, Journal of Engineering Materials and Technology, January, Vol. 113, pp. 31-40,1991.

16. Llorca, J., and Galvez, V. S., “Modeling Plasticity-induced Fatigue Crack Closure”, Engineering Fracture Mechanics, Vol. 37(1), pp. 185-196, 1990.

17. Tsukuda, H., Ogiyama, H., and Shiraishi, T., “Fatigue Crack Growth and Closure at High Stress Ratio. Fatigue and Facture in Engineering Materials and Structure, Vol. 18(4), pp. 503-514, 1995.

18. Shercliff, H. R., and Fleck, N. A., “Effect of Specimen Geometry on Fatigue Crack Growth in Plane Strain I - Constant Amplitude Response”, Fatigue and Facture in Engineering Materials and Structure, Vol. 13930, pp. 287-296,1990.

19. Shercliff, H. R., and Fleck, N. A., “Effect of Specimen Geometry on Fatigue Crack Growth in Plane Strain II - Overload Response.” Fatigue and Facture in Engineering Materials and Structure, Vol. 13(3), pp. 297-310, 1990.

20. Lalor, P., and Sehitoglu, H., “Fatigue Crack Closure Outside Small Scale Yielding Regime”, Mechanics of Fatigue Crack Closure. ASTM STP 982, pp. 342-360, 1988.

21. Solanki, K., Daniewicz, S. R., and Newman Jr., J. C., “Finite Element Modeling of Plasticity-Induced Crack Closure with Emphasis on Geometry and Mesh Refinement Effects”, Engineering Fracture Mechanics, Vol. 70 (12), pp.1475-1489,2003.

22. Solanki, K., Daniewicz, S. R., and Newman Jr., J. C., “A New Methodology for Computing Crack Opening Values from Finite Element Analyses”, Engineering Fracture Mechanics, Vol. 71 (7-8), pp.1165-1175, 2004.

23. Solanki K, Daniewicz S. R. and Newman, J. C., “Finite element analysis of plasticity-induced fatigue crack closure: an overview”, Engineering Fracture Mechanics, Vol. 71 (2), pp. 149-171, 2004 .

24. McClung, R. C., and Sehitoglu, H., “On the Finite Element Analysis of Fatigue Crack Closure-1: Basic Modeling Issues”, Engineering Fracture Mechanics, Vol. 33(2), pp. 237-252, 1983.

25. McClung, R. C., and Sehitoglu, H., “On the Finite Element Analysis of Fatigue Crack Closure-2: Numerical Results”, Engineering Fracture Mechanics, Vol. 33(2), pp. 253-272, 1983.

26. Ogura, K., and Ohji, K., “FEM Analysis of Crack Closure and Delay Effect in Fatigue Crack Growth Under Variable Amplitude Loading”, Engineering Fracture Mechanics, Vol. 9, pp. 471-480, 1977.

27. Ohji, K., Ogura, K., and Ohkubo, Y., “Cyclic Analyses of Propagating Crack and its Correlation with Fatigue Crack Growth”, Engineering Fracture Mechanics, Vol. 7, pp. 457-464, 1975.

28. McClung, R. C., “Closure and Growth of Mode I Cracks in Biaxial Fatigue”, Fatigue and Facture in Engineering Materials and Structure, Vol. 12(5), pp. 447-460, 1989.

29. McClung, R. C., “Finite Element Perspectives on the Mechanics of Fatigue Crack Closure”, Fatigue, pp. 345-356,1996.

30. Newman, J. C. Jr., “Finite-Element Analysis of Crack Growth Under Monotonic and Cyclic Loading”, ASTM STP 637, pp. 56-80,1977.

31. Wu, J., and Ellyin, F., “A Study of Fatigue Crack Closure by Elastic-Plastic Finite Element Analysis for Constant-Amplitude Loading”, International Journal of Fracture, Vol. 82, pp. 43-65,1996.

32. Park, S. J., Earmme, Y. Y., and Song, J.H., “Determination of the Most Appropriate Mesh Size for 2-D Finite Element Analysis of Fatigue Crack Closure Behavior”, Fatigue and Facture in Engineering Materials and Structure, Vol. 20(4), pp. 533-545, 1997.

33. McClung, R. C., “The Influence of Applied Stress, Crack Length, and Stress Intensity Factor on Crack Closure”, Metallurgical Transactions A, Vol. 22A, pp. 1559- 1571, July, 1991.

34. McClung, R. C., “Finite Element Analysis of Specimen Geometry Effects on Fatigue Crack Closure”, Fatigue and Facture in Engineering Materials and Structure, Vol. 17(8), pp. 861-872, 1994.

35. Nicholas, T., Palazotto, A., and Bednarz, E., “An Analytical Investigation of Plasticity Induced Closure Involving Short Cracks”, ASTM STP 982 pp. 361-379, 1988.

36. Blandford, R. S., Daniewicz, S. R., and Skinner, J. D., "Determination of the Opening Load for a Growing Crack: Evaluation of Experimental Data Reduction Techniques and Analytical Models", Fatigue and Facture in Engineering Materials and Structure, Vol. 25(1), pp.17-26, 2002.

37. Roychowdhury, S., and Dodds, Jr., R. H., "A Numerical Investigation of Three-Dimensional Small Scale-Yielding Fatigue Crack Growth", Engineering Fracture Mechanics, Vol. 70(17), pp. 2363-2383, 2003.

38. Roychowdhury, S., and Dodds, "Three-Dimensional Effects on Fatigue Crack Closure in the Small Scale-Yielding Regime – A Finite Element Study", Fatigue and Facture in Engineering Materials and Structure, Vol. 26(8), pp.663-673, 2003.

39. Chermahini, R. G., Shivakumar, K. N., and Newman, J. C., "Three-Dimensional Finite Element Simulation of Fatigue Crack Growth and Closure", ASTM STP 982, pp. 398-413, 1988.

40. Chermahini, R. G., Palmberg, B., and Blom, A. F., "Fatigue Crack Growth and Closure Behavior of Semi-Circular and Semi-Elliptical Surface Flaws", International Journal of Fatigue, Vol. 15(4), pp. 259-263, 1993.

41. Zhang, J. Z., and Bowen, P., "On the Finite Element Simulation of Three-Dimensional Semi-Circular Fatigue Crack Growth and Closure", Engineering Fracture Mechanics, Vol. 60, pp. 341-360, 1998.

42. Riddell, W. T., Piascik, R. S., Sutton, M. A., Zhao, W., McNeill, S. R., and Helm, J. D., "Determining Fatigue Crack Opening Loads From Near-Crack-Tip Displacement Measurements", ASTM STP 1343, Vol. 2, pp. 157-74, 1999.

43. Dawicke, D. S., Grandt, A. F. Jr., and Newman, J. C. Jr., "Three-Dimensional Crack Closure Behavior", Engineering Fracture Mechanics, Vol. 36(1), pp. 111-121, 1990.

44. Allison, J. E., Ku, R. C., and Pompetzki, M. A., "A Comparison of Measurement Methods and Numerical Procedures for the Experimental Characterization of Fatigue Crack Closure", ASTM STP 982, pp. 171-185, 1988.

45. Ray, S. K., and Grandt, A. F., Jr., "Comparison of Methods for Measuring Fatigue Crack Closure in a Thick Specimen", ASTM STP 982, pp. 197-213, 1988.

46. Donald, J. K., "A Procedure for Standardizing Crack Closure Levels", ASTM STP 982, pp. 222-229, 1988.

47. Daniewicz, S. R., and Bloom, J. M., "An Assessment of Geometry Effects on Plane Stress Fatigue Crack Closure Using a Modified Strip-Yield Model", International Journal of Fatigue, Vol. 18(7), pp.483-490, 1996.

48. Lee, H. J. and Song, J. H., "Finite Element Analysis of Fatigue Crack Closure Under Plane Strain Conditions: Stabilization Behaviour and Mesh Size Effects", Fatigue and Facture in Engineering Materials and Structure, Vol. 28, pp.333-342, 2005.

49. Nguyen, O., Repetto, E. A., Ortiz, M., and Radovitzky, R. A., "A Cohesive Model of Fatigue Crack Growth", International Journal of Fracture, Vol. 110, pp.351-369, 2001.

50. McClung, R. C. and Sehitoglu, H., "On the Finite Element Analysis of Fatigue Crack Closure-1. Basic Modeling Issues", Engineering Fracture Mechanics, Vol. 33, No. 2, 1989, pp.237- 252.

51. McClung, R. C. and Sehitoglu, H., "On the Finite ElementAnalysis of Fatigue Crack Closure-2. Numerical Results", Engineering Fracture Mechanics, Vol. 33, No. 2, 1989, pp.253-272.

52. Heper R. and Vardar O., "Elastic-plastic material response of fatigue crack surface profiles due to overload interactions", International Journal of Fatigue , Vol. 25 (9-11), pp. 801-810, 2003

53. ANSYS, User Manual, Elements, Vol.3, Revision 5.2, Houston, 1995.